Toral Marta (Orcid ID: 0000-0001-5324-8569)

Gómez-Guzmán Manuel (Orcid ID: 0000-0003-2452-9286)

Title: "Losartan-induced gut microbial changes has an antihypertensive effect"

Running title: Losartan restored gut microbiota in SHR

Iñaki Robles-Vera[1,*], Marta Toral[2,3*], Néstor de la Visitación[1], Manuel Sánchez[1,4], Manuel Gómez-Guzmán[1,4], Raquel Muñoz[1], Francesca Algieri[1,4], Teresa Vezza[1,4], Rosario Jiménez[1,3,4], Julio Gálvez[1,4], Miguel Romero[1,4], Juan Miguel Redondo[2,3], Juan Duarte[1,3,4,#]

[1]Department of Pharmacology, School of Pharmacy and Center for Biomedical Research (CIBM), University of Granada, 18071- Granada, Spain. [2]Gene Regulation in Cardiovascular Remodeling and Inflammation Group, Centro Nacional de Investigaciones Cardiovasculares (CNIC), Madrid, Spain. [3]Ciber de Enfermedades Cardiovasculares (CIBERCV), Spain. [4]Instituto de Investigación Biosanitaria de Granada, ibs.GRANADA, Granada, Spain.

 # Corresponding author: Juan Duarte. Department of Pharmacology, School of Pharmacy, University of Granada, 18071 Granada, Spain.

Phone: 0034958241791 Email: jmduarte@ugr.es

* I.R.V. and M.T. contributed equally as first authors

Word count: 4733

This article has been accepted for publication and undergone full peer review but has not been through the copyediting, typesetting, pagination and proofreading process which may lead to differences between this version and the Version of Record. Please cite this article as doi: 10.1002/bph.14965

Acknowledgments

This work was supported by Grants from Comisión Interministerial de Ciencia y Tecnología, Ministerio de Economía y competitividad (SAF2017-84894-R, SAF2014-55523-R, AGL2015-67995-C3-3-R), Junta de Andalucía (Proyecto de excelencia P12-CTS-2722, AGR-6826, and CTS-164) with funds from the European Union, and by the Ministerio de Economia y Competitividad, Instituto de Salud Carlos III (CIBER-CV; CIBER-EHD), Spain. M.T. is postdoctoral fellow of Sara Borrell. R.M. is postdoctoral fellow of CIBERCV. I.R.V. is a predoctoral fellow of MINECO. The cost of this publication was paid in part with funds from the European Union (Fondo Europeo de Desarrollo Regional FEDER). The authors acknowledge Nutraceutical Translations for English language editing of this manuscript.

Keywords: gut microbiota; hypertension; losartan; mesenteric lymph nodes.

Abstract

Background and Purpose: Hypertension is associated with gut dysbiosis. We aimed to evaluate the effects of the angiotensin receptor blocker losartan on gut microbiota in spontaneously hypertensive rats (SHR), and to test if this modification contributes to its blood pressure (BP) reducing properties.

Experimental Approach: Twenty-weeks old Wistar Kyoto rats (WKY) and SHR were assigned to three groups: untreated WKY (WKY), untreated SHR (SHR), and SHR treated with losartan for 5 weeks (SHR-losartan). A faecal microbiota transplantation (FMT) experiment was also performed by gavage of faecal content from donor SHR-losartan group to SHR recipient.

Key results: Faeces from SHR showed gut dysbiosis, characterised by higher *Firmicutes/Bacteroidetes* ratio, lower acetate- and higher lactate-producing bacteria, and lower strict anaerobic bacteria, which was restored by losartan. The improvement of gut dysbiosis was linked to higher colonic integrity and lower sympathetic drive in the gut. In contrast, hydralazine reduced BP but it did neither restore gut dysbiosis nor colonic integrity. Interestingly, FMT from SHR-losartan to SHR reduced BP, improved the aortic endothelium-dependent relaxation to acetylcholine and reduced NADPH oxidase activity. These vascular

changes were linked to both increased Treg and decreased Th17 cells population in the vascular wall.

Conclusions and Implications: Losartan treatment reduced gut dysbiosis in SHR. This effect seems to be related to its capacity to reduce sympathetic drive in the gut, improving gut integrity. The changes induced by losartan in gut microbiota contributed, at least in part, to protect the vasculature and reduce BP, possibly by modulating gut immune system.

Introduction

The gut harbours trillions of bacteria that modulate the host homeostasis within and outside the intestinal tract. Gut microbiota is commonly referred to as an essential acquired organ because its composition and richness are constantly adapting to the challenges occurring in the environment or in the host, such as age, diet, and lifestyle modifications. In addition, it has been commonly observed that a change in the host health status has been accompanied by a shift in the gut microbiota (Marques et al., 2017).

In the periphery, gut microbiota plays an important role in shaping a robust systemic and intestinal immune system (Chow et al., 2010; McDermott and Huffnagle, 2014). Recent data suggest that gut microbiota may also play a role in the development and maintenance of cardiovascular disease and metabolic disorders, such as obesity, diabetes mellitus, and metabolic syndrome (Tang et al., 2013; Tilg and Kaser A, 2011; Everard and Cani, 2013; Howitt and Garrett, 2012). Recently, it has been demonstrated that the normal gut microbiota may influence blood pressure (BP). A direct association between gut microbiota and hypertension in both animal models and humans has been described (Yang et al., 2015; Kim et al., 2018, Toral et al., 2019, Sun et al., 2019). In contrast, Karbach et al. (2016) showed that BP was not different between germ-free and conventionally raised mice, which is consistent with previous observations describing no effect on BP after dramatic reduction in faecal microbial biomass induced by antibiotic treatment (Pluznick et al., 2013). Similarly, it has been described that both the *Firmicutes*/*Bacteroidetes* (F/B) ratio and the abundance levels of selected genera in pre-hypertensive spontaneously hypertensive rats (SHR) were not significantly different from the age matched Wistar Kyoto rats (WKY) (Santisteban et al., 2016). Interestingly, transplantation of microbiota from SHR to WKY (Adnan et al., 2016, Toral et al, 2019a), or from hypertensive human to germ-free mice (Li et al., 2017) increased BP, showing the role of dysbiotic microbiota in the development of hypertension. In human, overgrowth of bacteria such as *Prevotella* and *Klebsiella,* have been described in both pre-

hypertensive and hypertensive populations as compared to healthy (Li et al., 2017). Moreover, seven bacterial species (*Parabacteroides johnsonii, Klebsiella unclassified, Anaerotruncus unclassified, Eubacterium siraeum, Prevotella bivia,* and *Rumminococcus torques*) positively, and three (*Bacteroides thetaiotaomicron, Paraprevotella clara,* and *Paraprevotella unclassified*) negatively correlacted with systolic BP (SBP) (Kim et al., 2018). In SHR, a strong positive correlation between SBP and the lactate-producing genus *Lactobacillus* (Adnan et al., 2017), or *Streptococcus* and *Turicibacter* (Yang et al., 2015, Toral et al., 2019b), and a negative correlation between butyrate-producing bacteria genus *Odoribacter* or acetate-producing bacteria genus *Bautia*, with SBP (Toral et al., 2019a) has been described. However, the absence of gut microbiota protects mice from angiotensin II-induced hypertension, vascular dysfunction, and hypertension-induced end-organ damage, showing for the first time that commensal microbiota, an ecosystem acquired after birth, could represent an environmental factor promoting angiotensin II-induced high BP (Karbach et al. 2016). Similarly, oral administration of antibiotics improved BP in angiotensin II-induced hypertension and in SHR (Yang et al., 2015). The BP reduction by minocycline was able to rebalance the hypertension-related dysbiotic gut microbiota by reducing the F/B ratio in angiotensin II-induced hypertension (Yang et al., 2015). Similarly, the consumption of probiotic *Lactobacillus* strains reduced BP in SHR (Gómez-Guzmán et al., 2015), in tacrolimus-induced hypertension in mice (Toral et al., 2018) and in high salt diet-induced hypertension in mice (Wilck et al., 2017), showing that restoring the microbiota composition to a similar composition as that found in normotensive animals led to the improvement of BP. In addition, increased permeability of gut epithelial barrier, intestinal inflammatory status and dysbiosis are associated with BP elevation in angiotensin II-infused mice (Kim et al., 2018). In fact, the inhibition of the renin-angiotensin system (RAS) by the angiotensin-converting enzyme (ACE) inhibitor captopril reduces BP, reverses gut pathology (Santisteban et al., 2017), and shifts the gut microbiota composition in SHR (Yang et al., 2019). However, whether BP reduction by other RAS inhibitors, such as the angiotensin receptor blocker losartan, shifts the gut microbiota composition is unclear. Whether changes in microbiota induced by these drugs are involved in their antihypertensive effects is also unknown.

Normal microbiota regulates immune homeostasis, such as the balance between T helper 17 (Th17) and regulatory T cells (Treg) in gut lymph organs and in the vascular wall, which is involved in BP regulation (Karbach et al., 2016; Toral et al., 2018). Furthermore, a critical role of the interaction gut microbiota-sympathetic nervous system in the regulation of BP has been recently described (Toral et al., 2019). We hypothesised that BP reduction in established hypertension might contribute to correct gut dysbiosis in SHR, which also contribute to maintain low BP through change T cell populations in the vascular wall.

Therefore, the aim of this study was to evaluate the effects of losartan on gut microbioma in SHR, and the role of gut microbiota in the antihypertensive effect of losartan.

Methods

Animals and experimental groups

This study was conducted in accordance with the regulations and requirements of the European Union concerning the protection of animals used for scientific purposes. The experimental protocol was approved by the Ethics Committee of Laboratory Animals of the University of Granada (Spain; permit number 03-CEEA-OH-2013). Animal studies are reported in compliance with the ARRIVE guidelines (McGrath and Lilley, 2015) and with the recommendations made by the British Journal of Pharmacology. Twenty weeks old male SHR/Kyo@Rj and WKY/Kyo@Rj from Envigo (RRID:RGD_5508396, Barcelona, Spain) were used in the present study. We selected SHR as an animal model of genetic hypertension. The SHR is a model with similar characteristics to essential hypertension in non-obese humans and one in which males have higher BP than females as young adults, but both sexes are hypertensive compared with normotensive Sprague-Dawley or WKY rats. Rats were kept in specific pathogen-free facilities at University of Granada Biological Services Unit. All animals were housed under standard laboratory conditions (12 hr light/dark cycle, temperature 21-22ºC, 50-70% humidity). Rats were housed in Makrolom cages (Ehret, Emmerdingen, Germany), with dust-free laboratory bedding and enrichment. In order to avoid horizontal transmission of the microbiota among animals, each rat was housed in a separate cage. Rats were provided with water and standard laboratory diet (SAFE A04, Augy, France) *ad libitum*. Water was changed every day, and both water and food intake was recorded daily for all groups. Studies were designed to generate groups of equal size. Animals were randomly assigned to treatment groups and the experimenter was blinded to drug treatment until data analysis has been performed.

Experiment 1: Rats were randomly assigned to three different experimental groups (n = 8): a) untreated WKY (WKY, 1 mL of tap water once daily), b) untreated SHR (SHR), and c) SHR treated with losartan (SHR-losartan, 20 mg kg^{-1} day^{-1} by oral gavage).

Experiment 2: SHR were randomly assigned to two groups (n = 8): a) SHR, and b) SHR treated with hydralazine (SHR-hydralazine, 25 mg kg^{-1} day^{-1} by oral gavage).

In both experiments, rats were treated for 5 weeks. Body weight was measured every week.

Experiment 3: To explore the role of microbiota from SHR-losartan group in the antihypertensive effects of losartan, a faecal microbiota transplantation (FMT) experiment was performed. For this purpose, faecal contents were collected fresh and pooled from individual rats from SHR and SHR-losartan groups at the end of the Experiment 1, twenty-four hours after the last dose of losartan. Twenty-week-old recipient SHR were orally gavaged with donor faecal contents for 3 consecutive days, and once every 3 days for a total period of 2 weeks. Animals were randomly assigned to two different groups of 8 animals each: SHR with SHR microbiota (S-S), and SHR with SHR-losartan microbiota (S-SLOS).

Faecal microbiota transplantation

The FMT to recipient rats was performed as previously reported (Toral et al., 2019). Faecal contents were diluted 1:20 in sterile PBS and centrifuged at 800 rpm for 5 minutes. The supernatant was aliquoted and stored at -80ºC. One week prior to transplantation, 1 mL ceftriaxone sodium (400 mg kg^{-1} day^{-1}) was administered daily to recipient rats for 5 consecutive days by oral gavage. Forty-eight hours after the last antibiotic treatment, recipient rats were orally gavaged with donor faecal contents (1 mL) as explained above. Losartan concentration in the supernatant used for FMT was measured by mass spectroscopy using previously published techniques (Okawada et al., 2011).

Blood pressure measurements

SBP and heart rate (HR) were measured weekly at room temperature using tail-cuff plethysmography as described previously (Vera et al., 2007). All experiments were performed in a quiet room by the same-blinded experimenter.

Cardiac and renal weight indices

When the experimental period was completed, 18 h fasting animals were anaesthetised with 2.5 mL kg^{-1} equitensin (i.p.) and blood was collected from the abdominal aorta. Finally, the rats were killed by exsanguination. The kidneys and the heart were then removed and

weighed. The heart was divided into right ventricle and left ventricle plus septum. All tissue samples were frozen in liquid nitrogen and then stored at -80ºC.

Plasma and colonic parameters

Blood samples were cooled on ice and centrifuged for 10 min at 3,500 rpm at 4ºC, and plasma was frozen at -80°C. Plasma lipopolysaccharide (LPS) concentration was measured using the Limulus Amebocyte Lysate chromogenic endotoxin quantitation Kit (Lonza, Valais, Switzerland), according to the manufacturer's instructions.

We used enzyme-linked immunosorbent assay kits (IBL International, Hamburg, Germany) to measure colonic noradrenaline (NA) concentrations following the manufacturer's protocol. Colon samples were collected and placed in the appropriate conservation solution. EDTA 1 mM and sodium metabisulfite 4 mM were added to prevent the catecholamine degradation. Then tissue samples were stored at -80ºC for later use.

Vascular reactivity studies

Segments of thoracic aortic rings (3 mm) were dissected from animals and were mounted in organ chambers filled with Krebs solution (composition in mM: NaCl 118, KCl 4.75, $NaHCO_3$ 25, $MgSO_4$ 1.2, $CaCl_2$ 2, KH_2PO_4 1.2 and glucose 11) as previously described (Gómez-Guzman et al., 2011).

The concentration-relaxation response curves to acetylcholine (10^{-9} -10^{-5} M) were studied in aorta pre-contracted using phenylephrine (1 μM) in the absence or the presence of N^G-nitro-L-arginine methyl ester (L-NAME, 100 μM) or apocynin (10 μM). The concentration-relaxation response curves to nitroprusside (10^{-9} -10^{-6} M) were performed in the dark in aortic rings without endothelium pre-contracted using 1 μM phenylephrine. Relaxation responses were expressed as a percentage of precontraction.

Measurement of *ex vivo* vascular reactive oxygen species (ROS) levels

We used dihydroethidium (DHE), an oxidative fluorescent dye, to localise ROS in aortic segments *in situ*, as previously described (Zarzuelo et al., 2011). Briefly, the aorta segments

were included in optimum cutting temperature compound medium (Tissue-Tek; Sakura Finetechnical, Tokyo, Japan), quickly frozen, and cut into 10 μm thick sections in a cryostat (Microm International Model HM500 OM). Sections were incubated at room temperature for 30 min with 10 μM DHE in the dark, counterstained with the nuclear stain 4,6-diamidino-2-phenylindole dichlorohydrate (DAPI, 300 nM) and in the following 24 h examined on a fluorescence microscope (Leica DM IRB, Wetzlar, Germany). Sections were photographed and ethidium and DAPI fluorescence were quantified using ImageJ (version 1.32j, NIH, http://rsb.info.nih/ij/). ROS production was estimated from the ratio of ethidium/DAPI fluorescence.

Immunofluorescent detection of macrophages and lymphocytes

Immunofluorescence microscopy was performed on 10-μm-thick cryostat aortic sections. Aortic sections were air-dried for 30 min, fixed for 5 min in methanol at -20˚C and washed with PBS for 15 min. Sections were blocked with PBS containing 5% non-fat dry milk for 2 h at room temperature and then incubated with a mouse anti-macrophage-specific antigen CD11b polyclonal antibody (1:200, Santa Cruz Biotechnology, Santa Cruz, USA), and a rabbit anti-CD3 polyclonal antibody (1:200, Abcam, Cambridge, UK) in blocking solution overnight at 4°C. The sections were washed 3 times with PBS and incubated with Alexa Fluor® 594 goat anti-rabbit, Alexa Fluor™ 488 goat anti-mouse (1:200, Molecular Probes, Oregon, USA) in the blocking solution for 1h at room temperature and then washed 3 times with PBS. Images were captured using a fluorescence microscope (Leica DM IRB, Wetzlar, Germany). The percentage of CD11 and CD3 staining/total surface area was quantified with Image J software (version 1.32j, NIH, http://rsb.info.nih/ij/) (Barhoumi et al., 2011).

NADPH oxidase activity

The lucigenin-enhanced chemiluminescence assay was used to determine NADPH oxidase activity in intact aortic rings as previously described (Zarzuelo et al., 2011). Aortic rings from all experimental groups were incubated for 30 minutes at 37ºC in HEPES-containing physiological salt solution (pH 7.4) of the following composition (in mM): NaCl 119, HEPES 20, KCl 4.6, $MgSO_4$ 1, Na_2HPO_4 0.15, KH_2PO_4 0.4, $NaHCO_3$ 1, $CaCl_2$ 1.2 and glucose 5.5. Then NADPH (100 μM) was added to the buffer containing the aortic rings, and lucigenin (5 μM) was injected automatically. NADPH oxidase activity was determined by measuring

luminescence over 200 s in a scintillation counter (Lumat LB 9507, Berthold, Germany) in 5-s intervals and was calculated by subtracting the basal values from those found in the presence of NADPH and expressed as RLU (relative light units)/min per mg of tissue for aortic rings.

Flow Cytometry

Mesenteric lymph nodes (MLNs) were collected from all groups. The tissues were mashed with wet slides to decrease friction and then the solutions were filtered through a 70µM cell strainer. 1×10^6 cells were counted and incubated with a protein transport inhibitor (BD GolgiPlugTM) for an optimum detection of intracellular cytokines by flow cytometry. For intracellular staining, cells were stimulated with 50 ng mL^{-1} phorbol 12-myristate 13-acetate plus 1 µg mL^{-1} ionomycin. After 4.5 hours, aliquot cells, of each sample, were blocked with anti-CD32 (clone D34-485) for 30 minutes at 4°C to avoid non-specific binding to Fc-gamma receptors. After that, cells were transferred to polystyrene tubes for the surface staining with mAbs anti-CD4 (PerCP-Vio700, clone REA482, Miltenyi Biotec, Bergisch Gladbach, Germany), anti-CD45 (APC, clone RA3-6B2 BD PharmigenTM, New Jersey, USA), and viability dye (LIVE/DEAD® Fixable Aqua Dead cell Sain Kit, Molecular Probes, Oregon, USA) for 20 min at 4°C in the dark. The lymphocytes were then fixed, permeabilised with the Fix/Perm Fixation/Permeabilisation kit (eBioscience, San Diego, USA) and intracellular staining was achieved with mAbs anti-forkhead box P3 (FoxP3) (PE,clone FJK-16s, eBioscience, San Diego, USA), anti-interleukin (IL)-17A (PE-Cy7, clone eBio17B7, eBioscience, San Diego, USA) and anti-IFNγ (Alexa Fluor® 647, DB-1, 6B2 BD Pharmigen™, New Jersey, USA) for 30 min at 4°C in the dark. All samples were analysed using a flow cytometer CANTO II (BD Biosciences) and data were analysed with FlowJo software (Tree Star, Ashland, OR, USA) (Romero et al., 2017).

Gene expression analysis

The analysis of gene expression was performed by reverse transcription polymerase chain reaction (RT-PCR), as previously described (Zarzuelo et al., 2011). For this purpose, total RNA was extracted by homogenisation using TRI Reagent® following the manufacturer's protocol. All RNA samples were quantified with the Thermo Scientific NanoDrop™ 2000 Spectrophotometer (Thermo Fisher Scientific, Inc., Waltham, MA, USA) and 2 µg of RNA

were reverse transcribed using oligo(dT) primers (Promega, Southampton, UK). Polymerase chain reaction was performed with a Techne Techgene thermocycler (Techne, Cambridge, UK). The sequences of the forward and reverse primers used for amplification are described in Table S1. The efficiency of the PCR reaction was determined using a dilution series of standard vascular samples. To normalise mRNA expression, the expression of the housekeeping gene β-actin was used. The mRNA relative quantification was calculated using the ΔΔCt method.

DNA Extraction, 16S rRNA Gene Amplification, Bioinformatics

For analysis of the bacterial population present in the gut, faecal samples were collected from six individual animals at the end of the experimental period. DNA was extracted from faecal samples using G-spin columns (INTRON Biotechnology) and starting from 30 mg of samples resuspended in PBS and treated with proteinase K and RNAses. DNA concentration was determined in the samples using Quant-IT PicoGreen reagent (Thermo Fischer), and DNA samples (about 3 ng) were used to amplify the V3-V4 region of 16S rRNA gene (Caporaso et al., 2011). PCR products (approx. 450 bp) included extension tails, which allowed sample barcoding and the addition of specific Illumina sequences in a second low-cycle number PCR. Individual amplicon libraries were analysed using a Bioanalyzer 2100 (Agilent) and samples were pooled in equimolar amounts. The pool was further cleaned, quantified and the exact concentration was estimated by real time PCR (Kapa Biosystems). Finally, DNA samples were sequenced on an Illumina MiSeq instrument with 2 x 300 bp paired-end sequencing reads at the Genomics Unit (Madrid Science Park, Spain).

We used the BIPES pipeline to process the raw sequences (Zhou et al., 2011). First, the barcode primers were trimmed and filtered if they contained ambiguous bases or mismatches in the primer regions according to the BIPES protocol. Second, we removed any sequences with more than one mismatch within the 40–70 bp region at each end. Third, we used 30 Ns to concentrate the two single-ended sequences for the downstream sequence analyses. A detailed description of these methods was previously reported (Liu et al., 2017). Third, we performed UCHIME (implemented in USEARCH, version 6.1) to screen out and remove chimeras in the *de novo* mode (using-minchunk 20-xn 7-noskipgaps 2) (Edgar and Flyvbjerg, 2015).

Between 90,000 and 220,000 sequences were identified in each sample. All subsequent analyses were performed using 16S Metagenomics (Version: 1.0.1.0) from Illumina. The sequences were then clustered to an operational taxonomic unit (OTU) using USEARCH with default parameters (USERACH61). The threshold distance was set to 0.03. Hence, when the similarity between two 16S rRNA sequences was 97%, the sequences were classified as the same OTU. QIIME-based alignments of representative sequences were performed using PyNAST, and the Greengenes 13_8 database was used as the template file. The Ribosome Database project (RDP) algorithm was applied to classify the representative sequences into specific taxa using the default database (Edgar and Flyvbjerg, 2015). The Taxonomy Database (National Center for Biotechnology Information) was used for classification and nomenclature. Bacteria were classified based on the short chain fatty acids (SCFAs) end-product as previously described (Wang et al., 2007; Antharam et al., 2013). Bacteria were classified based on the oxygen requirement using Genomes OnLine Database (GOLD) (Mukherjee et al., 2019).

Chemicals

All chemicals were obtained from Sigma-Aldrich (Barcelona, Spain), unless otherwise stated.

Statistical analysis

The data and statistical analysis comply with the recommendations on experimental design and analysis in pharmacology (Curtis et al., 2018). Statistical analysis was undertaken only for studies where each group size was at least n=5. Group size is the number of independent values, and statistical analysis was done using these independent values. The Shannon, Chao, Pielou and observed species indexes were calculated using QIIME (PAST 3x). Reads in each OTU were normalised to total reads in each sample. Only taxa with a percentage of reads > 0.001% were used for the analysis. Principal component analysis (PCA) was also applied to these data to identify significant differences between groups, using PAST 3x, and SSPS. Linear Discriminant Analysis (LDA) scores greater than 2 were displayed. Taxonomy was summarised at the genus level within QIIME-1.9.0 and uploaded to the Galaxy platform (Segata et al., 2011) to generate the LDA effect size (LEfSe)/cladogram enrichment plots considering significant enrichment at a $P<0.05$, LDA

score > 2. All data were analysed using GraphPad Prism 7 (RRID:SCR_000306). Results are expressed as means ± SEM of measurements. The evolution of tail SBP and the concentration-response curves to acetylcholine were analysed by two-way repeated-measures analysis of variance (ANOVA) with the Bonferroni *post hoc* test. The remaining variables were tested on normal distribution using Shapiro-Wilk normality test and compared using an unpaired t test or one-way ANOVA and Tukey *post hoc* test in case of normal distribution, or Mann-Whitney test or Kruskal-Wallis with Dunn's multiple comparison test in case of abnormal distribution. $P < 0.05$ was considered statistically significant.

Nomenclature of targets and ligands

Key protein targets and ligands in this article are hyperlinked to corresponding entries in http://www.guidetopharmacology.org, the common portal for data from the IUPHAR/BPS Guide to PHARMACOLOGY (Harding *et al.*, 2018), and are permanently archived in the Concise Guide to PHARMACOLOGY 2017/18 (Alexander *et al.*, 2017).

Results

Losartan treatment reduces gut dysbiosis in SHR

The compositions of bacterial communities were evaluated by calculating three major ecological parameters, including Chao richness, Pielou evenness, and Shannon diversity and the number of observed species. Reduced richness and diversity without changes in evenness and observed species were found in gut microbiota from SHR compared to those found in WKY. Losartan did not restore these changes despite its antihypertensive effect (Figure S1A).

We performed a three-dimensional PCA of the bacterial community, which measures microorganism diversity between samples, i.e. β-diversity, at the level of the different taxa (phylum, class, order, family, genus and species), in an unsupervised manner. This analysis at the phylum level showed a perfect clustering of the animals into the SHR and WKY groups, with no perfect clustering of the animals into SHR-losartan group (Figure S1B). The composition of the faecal microbial communities of the WKY and SHRs was found to be distinct from the previously reported composition (Yang et al., 2015). A clear separation was observed in the PCA between the 2 clusters representing the microbial compositions of WKY and SHR, indicating 2 extremely different gut environments. However, the cluster SHR-

losartan is closer to WKY than to SHR, being the key bacterial populations that are responsible for discriminating among groups the phylum *FIrmicutes* (loading 0.84). The Kaiser-Meyer-Olkin (KMO) test, that measure sampling adequacy, was 0,777, indicating a middling sampling. The Barlett's test of sphericity was < 0.05. The analysis of the phyla composition showed that *Firmicutes* was the most abundant phylum in the rat faeces, followed by *Proteobacteria*, *Actinobacteria, Bacteroidetes,* and *Verrucomicrobia* (Figure 1A). The proportion of bacteria from the *Fimicutes* phylum was significantly higher in SHR than in WKY and SHR-losartan, whereas the proportions of *Actinobacteria* and *Bacteroidetes* were lower in SHR than in the other groups. Losartan treatment restored bacteria from the *Firmicutes* and *Bacteroidetes* phyla to levels similar to those found in WKY. The F/B ratio, a signature of gut dysbiosis in hypertension (Yang et al., 2015), was ≈ 3-fold higher in SHR than in WKY, and this ratio returned to normal values by the action of losartan (Figure 1B). In addition, significant lower percentages of acetate- and propionate-producing bacteria, and a higher percentage of lactate-producing bacteria, without significant differences in the percentage of butyrate-producing bacteria, were found in SHR compared to WKY; these effects were abolished by losartan treatment (Figure 1C). Moreover, the percentage of strict anaerobic bacteria was significantly lower in SHR compared to WKY, no significant differences in strict aerobic bacteria were found between SHR and WKY. Losartan restored this change in the percentage of anaerobic bacteria (Figure 1D).

Figure S2 shows the bacterial taxa (class, order, family, and genus) that were altered in SHR according to LEfSe. Prominent changes in bacterial taxa occurred, where the relative abundance of 51 taxa was increased (green) and 19 taxa were decreased (red) in WKY compared to SHR. Losartan treatment of SHR also induced several changes in the microbiota taxa compared to SHR, where the relative abundance of 41 taxa was increased (green) and 16 taxa was decreased (red) (Figure S3).

We also identified what bacterial families (Figure S4) and genera (Figure S5) were associated with changes in the composition of microbiota. The key bacterial populations that are responsible for discriminating among groups was the familia *Clostridiaceae* (loading 0.38), and the genus *Oscillospira* (loading 0.78). The KMO test was 0,84, and 0,82, indicating in both cases a meritorious sampling for PCA at the family and genus levels, respectively. The Barlett's test of sphericity was < 0.05 in both cases. A significant depletion of *Verrucomicrobiacea, Pedobacter,* and *Akkermansia*, with a higher abundance of *Lactobacillaceae*, and *Lactobacillus* was found in the microbiota of SHR group compared to WKY. Losartan treatment tended to restore changes in *Verrucomicrobiacea, Pedobacter,* and *Akkermansia*, and significantly restored changes in *Lactobacillaceae and Lactobacillus*.

Losartan improved intestinal integrity, α-defensins production, gut sympathetic tone, and changed MLNs T cell population in SHR

Hypertension is associated with the altered expression of gut tight junction proteins, increased permeability and gut pathology. The ACE inhibitor captopril, which lowers BP in SHR, reverses gut pathology (Santisteban et al., 2017). We also found reduced mRNA levels of barrier-forming junction proteins (occludin and zonula occludens-1 (ZO-1)) in the colon of SHR compared to WKY (Figure 2A). Losartan treatment restored occludin and ZO-1 mRNA levels in the colon, suggesting an enhanced barrier function. In addition, increased gut permeability in adult hypertensive SHR correlates with reduced goblet cells (Santisteban et al., 2017). Goblet cells produce mucins, which protect the gut from pathogen invasion, thereby regulating gut immune response (Mowat AM, Agace WW, 2014). We have also found downregulation of mucin (MUC)-2 transcripts, without change in MUC-3 in SHR than in WKY, which was restored by losartan (Figure 2A), suggesting reduced gut permeability. We measured endotoxin levels in plasma, and found them to be significantly higher in SHR compared with the WKY group (Figure 2B). Interestingly, the long-term treatment with losartan significantly decreased endotoxemia in SHR. These results suggest that intestinal permeability is increased in SHR and allow bacterial components (e.g., LPS) to enter the blood stream. Furthermore, the increased mRNA levels of the colonic pro-inflammatory cytokines tumor necrosis factor-α (TNF-α) and IL-6 (Figure 2C) in SHR were significantly reduced by losartan administration.

RAS participates in the regulation of gastrointestinal inflammation (Garg et al., 2012; Brzozowski, 2014) and has been linked to human inflammatory bowel diseases (IBD) (Hume et al., 2016). In fact, pharmacological inhibition of classical RAS with losartan is capable to alleviate murine models of IBD, independently of their antihypertensive effects (Wengrower et al., 2012; Liu et al, 2016). However, we did not found any changes in the mRNA levels of several RAS components, such as angiotensinogen (AGT), ACE and ACE2 (Figure 3A), in colonic samples from all experimental groups, suggesting that the protective effects of losartan in both colonic integrity and inflammation seems to be independent of local RAS inhibition. Santisteban et al., (2017) showed that the increase in the sympathetic nerve activity to the gut lead to alteration of gut junction proteins in SHR. We found an increase in the expression of tyrosine hydroxylase (TH), a key enzyme involved in NA generation and NA content in the gut from SHR compared to WKY, which was abolished by chronic losartan

treatment (Figure 3B). These results suggest that reduced sympathetic tone in the gut could be involved in the protective effects of losartan in the gut.

Epithelial intestinal cells are able to secrete antimicrobial peptides, α-defensins, which are cysteine-rich cationic peptides with antibiotic activity against a wide range of bacteria and other microbes (Bevins, 2005), to maintain the intestinal microbiota composition (Hashimoto et al., 2012). We found reduced mRNA levels of the α-defensin RNP1-2, and increased mRNA levels of RNP3 and RNP4, without significant change of RNP5 in colon from SHR compared to the WKY group. Again, losartan treatment restored the mRNA levels of defensins to levels similar to those found in WKY (Figure 3C).

Under altered gut mucosal integrity, bacteria are able to translocate across the intestinal epithelium leading to activation and migration of CX3CR1^{+} cells, such as macrophages and dendritic cells, to draining lymph nodes of the lower intestinal tract (Niess et al., 2005). They also present soluble antigen to naïve CD4+ T cells, leading to T cell activation. We found that the number of total lymphocytes in MLNs was higher in SHR compared to WKY (Figure 4). Losartan treatment did not change the content in lymphocytes in MLNs. The percentage of Treg ($CD4^{+}/FoxP3^{+}$) was reduced, whereas the percentage of Th17 ($CD4^{+}/IL\text{-}17^{+}$) lymphocytes was significantly increased in MLNs in SHR compared to WKY (Figure 4). Losartan increased only Treg population in MLNs without affecting Th17 population.

Losartan reduces blood pressure and organ target damage and improves vascular nitric oxide (NO) pathway, oxidative stress and inflammation

As expected, SHR receiving chronic losartan treatment showed a progressive decrease in SBP (Figure S6A), which was already significant after the first week, and was almost normalised after 5 weeks (a decrease of 54.7 ± 9.4 mmHg). No significant differences were found among groups in heart rate (not shown). At the end of the study period, losartan prevented the increase in the left ventricular weight index (≈ 12 %) and in urine protein excretion (≈ 51 %) found in SHR compared with the WKY counterparts (data not shown).

Aortas from the SHR control group showed strongly reduced endothelium-dependent vasodilator responses to acetylcholine compared to aortas from the WKY group, which was restored after losartan treatment (Figure S6B). The incubation with L-NAME in the organ bath abolished the relaxation response to acetylcholine in all experimental groups, involving

NO in this relaxation (data not shown). The presence of the non-selective NADPH oxidase inhibitor apocynin in the organ bath increased the relaxation response to acetylcholine in untreated SHR until reaching similar relaxation percentages to those found in WKY (Figure S6B), suggesting that an increased NADPH oxidase activity is involved, at least in part, in the impaired relaxation to acetylcholine in aorta from SHR. In addition, no differences were observed among groups in the endothelium-independent vasodilator responses to the NO donor sodium nitroprusside in aortic rings, excluding changes in NO pathway in smooth muscle (data not shown). Rings from SHR showed both marked increased ROS content (Figure S6C), measured by red staining to ethidium in vascular wall (≈ 27 %), and NADPH oxidase activity (Figure S6D) compared to WKY, which were suppressed by losartan.

The infiltration of T cells and macrophages measured by immunofluorescence was higher in aorta from SHR than from WKY counterparts, and was inhibited by losartan (Figure 5A). In addition, we also analysed the transcript level of transcription factor FoxP3, retinoid-related orphan receptor-γ (RORγ), T-bet and GATA3, as markers of accumulation of Treg, Th17, Th1 and Th2, respectively, in aorta from all experimental groups (Figure 5B). Aortic Th17, Th1, and Th2 contents were increased in SHR group, whereas Treg content was reduced. Aorta from the SHR-losartan group showed levels of T cells similar to those found in WKY (Figure 5B). The mRNA expression of pro-inflammatory cytokines IL-17a, IFN-γ and TNF-α was higher, whereas the mRNA levels of anti-inflammatory IL-10 were lesser in aortic homogenates from SHR than in WKY. Losartan treatment significantly suppressed these changes (Figure 5C).

Hydralazine reduced blood pressure, cardiac hypertrophy and improved endothelial function, but did not restore gut microbiota and gut integrity.

To differentiate between the effects of blocking AT1 receptors *vs.* lowering arterial pressure, the effect of hydralazine, another vasodilator-acting antihypertensive drug, on gut microbiota was tested. This drug also reduced SBP, being significant at the first week of treatment and reaching a decrease of 73.4 ± 7.6 mm Hg after 5 weeks, similar to that induced by losartan (Figure 6A). In contrast, hydralazine significantly increased heart rate (Figure 6B), suggesting increased sympathetic activity. Hydralazine treatment also reduced left ventricular hypertrophy (Figure 6C), improved the endothelium-dependent relaxation to acetylcholine (Figure 6D) and reduced the vascular NADPH oxidase activity (Figure 6E).

The composition of bacterial community was evaluated. The major ecological parameters were not altered by hydralazine treatment. Only a reduced Shannon diversity was found in SHR-hydralazine group compared to SHR (Figure 7A). An unclear separation was observed in the PCA between the 2 clusters representing the microbial compositions of SHR and SHR-hydrazine groups, indicating 2 similar gut environments (Figure 7B). The key bacterial populations that are responsible for discriminating among groups was the phylum *Bacteroidetes* (loading 0.74). The KMO test was 0,71, indicating a middling sampling. The Barlett's test of sphericity was < 0.05. In addition, the proportion of bacteria among phyla (Figure 7C), the F/B ratio (Figure 7D), the proportion SCFAs-producing bacteria (Figure 7E), and the percentage of strict anaerobic bacteria (Figure 7F) were similar between both groups, showing that hydralazine did not alter gut dysbiosis, despite its antihypertensive effect.

In the gut, hydralazine was unable to change the mRNA levels of the RAS components (data not shown), but it increased the TH expression and the NA content (Figure 8A), suggesting higher colonic sympathetic drive. In addition, no significant modifications were induced by hydralazine in mRNA levels of barrier-forming junction proteins and mucins (Figure 8B), showing that this drug did no improve gut integrity. Furthermore, colonic α-defensins expression was not restored by hydralazine (Figure 8C).

Faecal microbiota transplantation (FMT) from SHR-losartan reduces blood pressure and improves endothelial function in SHR

To test if changes in gut microbiota composition induced by a chronic treatment with losartan were involved in their antihypertensive effects, a FMT from SHR treated with losartan to SHR was performed, and compared to FMT from an untreated SHR to another untreated SHR. We found a significant decrease of 16.6 ± 7.0 mm Hg in SBP after 2 weeks of FMT from SHR-Losartan to SHR, whereas no changes in SBP were found when FMT was performed from SHR to SHR (Figure 9A). In addition, an improvement of the endothelium-dependent relaxation to acetylcholine (Figure 9B) and a reduced NADPH oxidase activity (Figure 9C) were also induced by stool transplantation from SHR treated with losartan. These vascular changes were linked to both increased Treg and decreased Th17 cells population in the vascular wall (Figure 9D). In addition, FMT from SHR-losartan to SHR increased colonic ZO-1, and MUC-2 expression (Figure 10A) and reduced colonic TH mRNA level (Figure 10B), suggesting improvement of gut integrity and gut sympathetic tone. In addition, increased Tregs cells in MLNs were detected in S-SLOS group compared to S-S

(Figure 10C), indicating that microbiota from SHR treated with losartan induced positive changes in this secondary lymph organ in the gut.

It has been reported that 60% losartan can be found in faeces and the donor samples could contain the drug. However, a low concentration of 0.60 µg/mL of losartan was detected in faeces from SHR-Losartan group, which rendered a losartan dose of 0.15 µg Kg^{-1} excluding that the observed effects in S-SLOS group were related to direct actions of the drug. As expected, losartan were not detected in faecal samples from untreated SHR.

At the end of the experiment the composition of faecal microbiota was analysed. The bacterial communities evaluated by calculating major ecological parameters (Chao richness, Pielou evenness, Shannon diversity and the number of observed species), were similar between both groups (data not shown). The proportion of bacteria from the *Fimicutes* and *Verrucomicrobia* phyla was significantly lower, whereas the proportions of *Bacteroidetes* were higher in S-SLOS than in S-S group (Figure S7A). The F/B ratio was also lower in S-SLOS group (Figure S7B). In addition, significant lower percentages of lactate- and propionate-producing bacteria, and a higher percentage of acetate-producing bacteria, were found in S-SLOS compared to S-S (Figure S7C). Moreover, the percentage of strict anaerobic bacteria was significantly higher in S-SLOS compared to S-S (Figure S7D).

Figure S8 shows the bacterial taxa that prominent changes in bacterial taxa occurred, where the relative abundance of 30 taxa was increased (green) and 64 taxa were decreased (red) in S-SLOS compared to S-S. A clear separation was observed in the PCA between the 2 clusters representing the microbial compositions of S-S and S-SLOS groups (Figure S9A). The key bacterial populations that are responsible for discriminating among groups the genus *Bacteroides* (loading 0.56). The KMO test was 0,84, indicating a meritorious sampling. The Barlett's test of sphericity was < 0.05. Bacterial genera were associated with changes in the composition of microbiota (Figure S9B). A significant reduction of *Oscillospira*, with a higher abundance of *Bacteroides, Prevotella and Clostridium* was found in the microbiota of S-SLOS group compared to S-S (Figure S9C). Interestingly, increased proportion of *Bacteroides acidifaciens* was detected as main strain in S-SLOS group (Figure S9D).

Discussion and conclusions

The main new findings of this study are the following: 1) chronic losartan treatment reduces gut dysbiosis in SHR; 2) changes in gut microbiota composition induced by losartan are independent of its BP reducing effects, and seem to be related to improvement of gut integrity and the normalisation of colonic α-defensins production, as a result of reduced gut sympathetic drive; 3) microbiota SHR-losartan is able to improve gut integrity, aortic endothelial dysfunction and reduce BP in rats with genetic hypertension.

Abundant evidence has demonstrated the association between gut dysbiosis and hypertension (Mell et al*.,* 2015; Yang et al*.,* 2015, Li et al 2017, Toral et al., 2019; Sun et al., 2019). Our results are consistent with the main features of dysbiotic microbiota described in SHR (Yang et al., 2015; Toral et al., 2019, Yang et al., 2019): a) a reduced richness and diversity, b) an increased F/B ratio, and c) a reduction in acetate- and propionate-producing bacteria, with higher proportion of lactate-producing bacteria. Losartan treatment tended to increase richness and diversity, whereas separated bacteria clusters from SHR towards WKY, normalised F/B ratio and SCFAs-producing bacteria. The increased abundance of *Lactobacillus ssp.* found in SHR samples was also normalised. All these changes induced by losartan in microbiota were linked to reduced BP, improvement of left ventricle hypertrophy, reduced both vascular oxidative status and accumulation of pro-inflammatory lymphocytes, and improvement of endothelial dysfunction.

Losartan may elicit changes in gut microbiota by several mechanisms. It has been commonly observed that a change in the host health status has been accompanied by a shift in the gut microbiota. Therefore, microbiota could be adapted to BP reduction, shifting to a microbiota composition similar to WKY. However, our results are contrary to this hypothesis because hydralazine, which reduced BP in a similar extent to losartan, was unable to alter dysbiosis in SHR. Changes in gut microbiota composition have been associated with gut integrity (Kim et al, 2018). The mammalian digestive tract epithelial cells create a tight barrier in the gut, contributing to the hypoxic environment of the lumen. Damage to this barrier makes the environment less hypoxic, conducive to aerobic bacterial growth (Konig et al., 2016; Earley et al, 2015). In fact, intestines of angiotensin II-hypertensive mice were significantly less hypoxic and with increased aerobic bacteria in faeces (Kim et al., 2018). We also found decreased abundance of anaerobic bacteria in faeces from SHR, which was associated with lost of gut integrity. SHR treated with losartan showed increase colonic integrity and a proportion of strict anaerobic bacteria similar to WKY, whereas hydralazine was unable to improve both gut integrity and the proportion of anaerobic bacteria. This data

support the key role of gut integrity in the composition of intestinal microbiota. In addition, intestinal epithelial cells and Paneth cells secrete antimicrobial peptides, such as defensins, which selectively kill Gram-positive bacteria (Pamer, 2007; Ayabe et al., 2000; Vora et al, 2004; Vaishnava et al., 2008). Components of the microbiota, such as LPS, are recognized by Toll-like Receptors expressed by these intestinal cells and trigger production and secretion of these defensins. We found changes in mRNA levels of defensins in colonic samples from SHR compared to WKY, which might also be involved in changes in microbiota found in this hypertensive rats. Losartan restored defensins expression to become similar to that found in WKY, whereas hydralazine did not altered the expression of RNP1-2 and RPN3 and enhanced the increased expression of RNP4 found in SHR, suggesting a role of defensins in the different changes in gut microbiota induced by both drugs.

Angiotensin receptor blockers have gut anti-inflammatory properties via inhibition of angiotensin II/ angiotensin II type 1 receptor (AT1) axis (Takeshita and Murohara, 2014). Inhibition of the classical RAS pathway is also involved in the upregulation of ACE2, which activates the Ang-(1-7)/Mas pathway to counteract inflammatory signaling (Yisireyili et al., 2018). In our study, no significant changes in AGT, ACE and ACE2 expression were found among colonic samples from WKY, SHR and SHR-losartan groups ruling out that changes in this pathway were involved in the protective effects of losartan in gut integrity. Our current study is consistent with Santisteban et al., (2017), demonstrating an increased gut sympathetic drive (increased TH expression and NA accumulation) associated with lost of gut integrity and microbial dysbiosis in SHR. Recently, the hypothesis posing the presence of a brain-gut communication driven by sympathetic system has been reinforced. Central administration of a modified tetracycline inhibited microglial activation, normalised sympathetic activity, attenuated pathological alterations in gut wall, restored certain gut microbial communities altered by angiotensin II and reduced BP (Sharma et al., 2019). Our data also support that gut sympathetic drive is a key regulator of gut integrity and microbiota composition. It is pertinent to note that sympathetic tone in SHR is attenuated by RAS-inhibition (Tsuda et al., 1988, Demirci et al., 2005; Santisteban et al., 2017), and increased by hydralazine (Tsoporis and Leenen, 1988). In fact, losartan treatment reduced sympathetic activity in the colon, improving gut integrity and reducing gut dysbiosis, whereas hydralazine (that increased gut sympathetic drive) was unable to restore gut integrity and microbiota composition.

Normal microbiota could regulate immune system and/or gut-brain communication reducing BP. In fact, Karbach et al (2016), showed that angiotensin II infusion to germ-free mice reduced ROS formation in the vasculature, attenuated vascular expression of NADPH oxidase subunit Nox2, and reduced upregulation of RORγ, the signature transcription factor for IL-17 synthesis in the aortic vessel wall. These vascular changes exerted protection from endothelial dysfunction and attenuation of BP increase in response to angiotensin II, involving immune system in the effects of microbiota in vascular function and BP regulation. We have recently described that FMT from WKY to SHR reduced neuroinflammation, sympathetic nervous system activity and BP (Toral et al., 2019a). In addition, the antihypertensive effect of the ACE inhibitor captopril has sustained influence on the brain-gut axis even after the withdrawal of captopril (Yang et al., 2019). When we explore the effects of FMT from donors SHR-losartan to receptors SHR, we found decreased F/B ratio, thus improving gut dysbiosis, and increased the prevalence of acetate-producing bacteria and those of the genus *Bacteroides acidifaciens*. This bacterium was recently associated to reduced SBP in DOCA-salt hypertension (Marques et al., 2017). In addition, it shown to prevent obesity and to improve insulin sensitivity in mice (Yang et al., 2017), but whether it can prevent the development of high BP in monocolonized animal is yet to be determined. These changes in gut microbiota were accompanied by a reduced BP, an improvement of endothelial dysfunction, a reduction of aortic NADPH oxidase activity linked to increased aortic Tregs infiltration without changes in Th17. IL-10, the main cytokine released by Tregs, attenuates NADPH oxidase activity, which is a critical process in the improvement of vascular endothelial function in hypertension (Kassan et al., 2011). The changes in T cell infiltration in the vascular wall were similar to that found in MLNs, suggesting that a regulation in T cell population in this gut secondary lymph organ by microbiota is involved in the antihypertensive effects of losartan. In fact, microbial metabolites, such as acetate, derived from acetate-producing bacteria in S-SLOS, might promote T-cell differentiation into Tregs cells (Park et al., 2015), leading to reduced BP.

In conclusion, we have found for the first time that losartan treatment reduced gut dysbiosis in SHR. This effect seems to be related to its capacity to reduce sympathetic drive in the gut, improving gut integrity and defensins production. The changes induced by losartan in gut microbiota contributed, at least in part, to protect the vasculature and reduce BP, possibly by modulating gut immune system (Figure S10). No sex-differences have been described in the antihypertensive effects of angiotensin receptor antagonists in humans. However, if the effects of losartan are sex-independent deserves further investigation in female SHR.

Conflict of interest

The authors declare no conflict of interest

Declaration of transparency and scientific rigour

This Declaration acknowledges that this paper adheres to the principles for transparent reporting and scientific rigour of preclinical research as stated in the *BJP* guidelines for Design & Analysis, and Animal Experimentation, and as recommended by funding agencies, publishers and other organisations engaged with supporting research.

Author contributions

J.D. conceived and designed the research; I.R.V, M.T., N.V.P., M.S., M.G.G., R.M., F.A. and M.R. performed the experiments and analysed the data; R.J., J.G., J.M.R. and J.D. interpreted the results; I.R.V, M.T. and R.J. prepared figures; J.D. drafted this manuscript; I.R.V, M.T., R.J., J.G., J.M.R. and J.D. edited and revised the manuscript; All authors approved the final version of manuscript.

Abbreviations

ACE, angiotensin-converting enzyme; AGT, angiotensinogen; AT1, angiotensin II type 1 receptor; BP, blood pressure; DAPI, 4,6-diamidino-2-phenylindole dichlorohydrate; DHE, dihydroethidium; F/B*, Firmicutes*/*Bacteroidetes*; FMT, faecal microbiota transplantation; FoxP3, forkhead box P3; GOLD; Genomes OnLine Database; HR, heart rate; IBD, inflammatory bowel diseases; IL, interleukin; KMO, Kaiser-Meyer-Olkin; L-NAME, N^G-nitro-L-arginine methyl ester; LDA, Linear Discriminant Analysis; LPS, lipopolysaccharide; MLNs, mesenteric lymph nodes; MUC, mucin; NA, noradrenaline; NO, nitric oxide; OTU, operational taxonomic unit; PCA, three-dimensional principal component analysis; PLS, Partial Least Square; RAS, renin-angiotensin system; RDP, Ribosome Database project; RORγ, retinoid-related orphan receptor-γ; ROS, reactive oxygen species; SBP, systolic

blood pressure; SCFAs, short chain fatty acids; SHR, spontaneously hypertensive rats; Th, T helper; TH, tyrosine hydroxylase; TNF-α, tumor necrosis factor-alpha; Treg, regulatory T cells; WKY, Wistar Kyoto rats; ZO-1, zonula occludens-1.

Bullet point summary:

'What is already known'

Gut microbiota is involved in the control of BP. RAS inhibition reduces BP, reverses gut pathology, and shifts the gut microbiota composition in SHR.

'What this study adds'

RAS inhibition corrects gut dysbiosis due to its capacity to inhibit sympathetic drive, leading to improvement of gut integrity. These changes in gut microbiota contributed to the reduction of BP.

'Clinical significance'

Gut microbiota represent a new target for losartan in the BP control. The gut dysbiosis inhibition by antihypertensive drugs might be involved in lower BP in genetic hypertension.

References

Adnan, S., Nelson, J. W., Ajami, N. J., Venna, V. R., Petrosino, J. F., Bryan, R. M., Jr., & Durgan, D. J. (2017). Alterations in the gut microbiota can elicit hypertension in rats. Physiol Genomics, 49(2), 96-104. doi:10.1152/physiolgenomics.00081.2016

Alexander SPH, Fabbro D, Kelly E, Marrion NV, Peters JA, Faccenda E., . . . CGTP Collaborators (2017). The Concise Guide to PHARMACOLOGY 2017/18: Enzymes. Br J Pharmacol. 174 Suppl 1: S272–S359.

Ayabe, T., Satchell, D. P., Wilson, C. L., Parks, W. C., Selsted, M. E., & Ouellette, A. J. (2000). Secretion of microbicidal alpha-defensins by intestinal Paneth cells in response to bacteria. Nat Immunol, 1(2), 113-118. doi:10.1038/77783

Barhoumi, T., Kasal, D. A., Li, M. W., Shbat, L., Laurant, P., Neves, M. F., . . . Schiffrin, E. L. (2011). T regulatory lymphocytes prevent angiotensin II-induced hypertension and vascular injury. Hypertension, 57(3), 469-476. doi:10.1161/HYPERTENSIONAHA.110.162941

Bevins, C. L. (2005). Events at the host-microbial interface of the gastrointestinal tract. V. Paneth cell alpha-defensins in intestinal host defense. Am J Physiol Gastrointest Liver Physiol, 289(2), G173-176.

Brzozowski, T. (2014). Role of renin-angiotensin system and metabolites of angiotensin in the mechanism of gastric mucosal protection. Curr Opin Pharmacol, 19, 90-98. doi:10.1016/j.coph.2014.08.007

Caporaso, J. G., Lauber, C. L., Walters, W. A., Berg-Lyons, D., Lozupone, C. A., Turnbaugh, P. J., . . . Knight, R. (2011). Global patterns of 16S rRNA diversity at a depth of millions of sequences per sample. Proc Natl Acad Sci U S A, 108 Suppl 1, 4516-4522. doi:10.1073/pnas.1000080107

Chow, J., Lee, S. M., Shen, Y., Khosravi, A., & Mazmanian, S. K. (2010). Host-bacterial symbiosis in health and disease. Adv Immunol, 107, 243-274. doi:10.1016/B978-0-12-381300-8.00008-3

Curtis, M.J., Alexander, S., Cirino, G., Docherty, J.R., George, C.H., Giembycz, M.A., . . . Ahluwalia, A. (2018). Experimental design and analysis and their reporting II: updated and simplified guidance for authors and peer reviewers. Br. J. Pharmacol. 175, 987-993. doi:10.1111/bph.14153

Eid, B.G., Gurney, A.M., 2018. Zinc pyrithione Demirci, B., McKeown, P. P., & Bayraktutan, U. (2005). Blockade of angiotensin II provides additional benefits in hypertension- and ageing-related cardiac and vascular dysfunctions beyond its blood pressure-lowering effects. J Hypertens, 23(12), 2219-2227.

Earley, Z. M., Akhtar, S., Green, S. J., Naqib, A., Khan, O., Cannon, A. R., . . . Choudhry, M. A. (2015). Burn Injury Alters the Intestinal Microbiome and Increases Gut Permeability and Bacterial Translocation. PLoS One, 10(7), e0129996. doi:10.1371/journal.pone.0129996

Edgar, R. C., & Flyvbjerg, H. (2015). Error filtering, pair assembly and error correction for next-generation sequencing reads. Bioinformatics, 31(21), 3476-3482. doi:10.1093/bioinformatics/btv401

Everard, A., & Cani, P. D. (2013). Diabetes, obesity and gut microbiota. Best Pract Res Clin Gastroenterol, 27(1), 73-83. doi:10.1016/j.bpg.2013.03.007

Garg, M., Angus, P. W., Burrell, L. M., Herath, C., Gibson, P. R., & Lubel, J. S. (2012). Review article: the pathophysiological roles of the renin-angiotensin system in the gastrointestinal tract. Aliment Pharmacol Ther, 35(4), 414-428. doi:10.1111/j.1365-2036.2011.04971.x

Gomez-Guzman, M., Jimenez, R., Sanchez, M., Romero, M., O'Valle, F., Lopez-Sepulveda, R., . . . Duarte, J. (2011). Chronic (-)-epicatechin improves vascular oxidative and inflammatory status but not hypertension in chronic nitric oxide-deficient rats. Br J Nutr, 106(9), 1337-1348. doi:10.1017/S0007114511004314

Gomez-Guzman, M., Toral, M., Romero, M., Jimenez, R., Galindo, P., Sanchez, M., . . . Duarte, J. (2015). Antihypertensive effects of probiotics Lactobacillus strains in

spontaneously hypertensive rats. Mol Nutr Food Res, 59(11), 2326-2336. doi:10.1002/mnfr.201500290

Harding SD, Sharman JL, Faccenda E, Southan C, Pawson AJ, Ireland S., . . . NC-IUPHAR (2018). The IUPHAR/BPS Guide to PHARMACOLOGY in 2018: updates and expansion to encompass the new guide to IMMUNOPHARMACOLOGY. Nucl Acids Res 46: D1091-D1106.

Hashimoto, T., Perlot, T., Rehman, A., Trichereau, J., Ishiguro, H., Paolino, M., . . . Penninger, J. M. (2012). ACE2 links amino acid malnutrition to microbial ecology and intestinal inflammation. Nature, 487(7408), 477-481. doi:10.1038/nature11228

Howitt, M. R., & Garrett, W. S. (2012). A complex microworld in the gut: gut microbiota and cardiovascular disease connectivity. Nat Med, 18(8), 1188-1189. doi:10.1038/nm.2895

Hume, G. E., Doecke, J. D., Huang, N., Fowler, E. V., Brown, I. S., Simms, L. A., & Radford-Smith, G. L. (2016). Altered Expression of Angiotensinogen and Mediators of Angiogenesis in Ileal Crohn's Disease. J Gastrointestin Liver Dis, 25(1), 39-48. doi:10.15403/jgld.2014.1121.251.chr

Karbach, S. H., Schonfelder, T., Brandao, I., Wilms, E., Hormann, N., Jackel, S., . . . Wenzel, P. (2016). Gut Microbiota Promote Angiotensin II-Induced Arterial Hypertension and Vascular Dysfunction. J Am Heart Assoc, 5(9). doi:10.1161/JAHA.116.003698

Kim, S., Goel, R., Kumar, A., Qi, Y., Lobaton, G., Hosaka, K., . . . Raizada, M. K. (2018). Imbalance of gut microbiome and intestinal epithelial barrier dysfunction in patients with high blood pressure. Clin Sci (Lond), 132(6), 701-718.doi:10.1042/CS20180087

Konig, J., Wells, J., Cani, P. D., Garcia-Rodenas, C. L., MacDonald, T., Mercenier, A., . . . Brummer, R. J. (2016). Human Intestinal Barrier Function in Health and Disease. Clin Transl Gastroenterol, 7(10), e196. doi:10.1038/ctg.2016.54

Li, J., Zhao, F., Wang, Y., Chen, J., Tao, J., Tian, G., . . . Cai, J. (2017). Gut microbiota dysbiosis contributes to the development of hypertension. Microbiome, 5(1), 14. doi:10.1186/s40168-016-0222-x

Liu, T. J., Shi, Y. Y., Wang, E. B., Zhu, T., & Zhao, Q. (2016). AT1R blocker losartan attenuates intestinal epithelial cell apoptosis in a mouse model of Crohn's disease. Mol Med Rep, 13(2), 1156-1162. doi:10.3892/mmr.2015.4686

Liu, Z., Liu, H. Y., Zhou, H., Zhan, Q., Lai, W., Zeng, Q., . . . Xu, D. (2017). Moderate-Intensity Exercise Affects Gut Microbiome Composition and Influences Cardiac Function in Myocardial Infarction Mice. Front Microbiol, 8, 1687. doi:10.3389/fmicb.2017.01687

Marques, F. Z., Nelson, E., Chu, P. Y., Horlock, D., Fiedler, A., Ziemann, M., . . . Kaye, D. M. (2017). High-Fiber Diet and Acetate Supplementation Change the Gut Microbiota and Prevent the Development of Hypertension and Heart Failure in Hypertensive Mice. Circulation, 135(10), 964-977. doi:10.1161/CIRCULATIONAHA.116.024545

McDermott, A. J., & Huffnagle, G. B. (2014). The microbiome and regulation of mucosal immunity. Immunology, 142(1), 24-31. doi:10.1111/imm.12231

McGrath, J. C., & Lilley, E. (2015). Implementing guidelines on reporting research using animals (ARRIVE etc.): new requirements for publication in BJP. *British journal of pharmacology*, *172*(13), 3189-3193.

Mell, B., Jala, V. R., Mathew, A. V., Byun, J., Waghulde, H., Zhang, Y., . . . Joe, B. (2015). Evidence for a link between gut microbiota and hypertension in the Dahl rat. Physiol Genomics, 47(6), 187-197. doi:10.1152/physiolgenomics.00136.2014

Mowat, A. M., & Agace, W. W. (2014). Regional specialization within the intestinal immune system. Nat Rev Immunol, 14(10), 667-685. doi:10.1038/nri3738

Mukherjee, S., Stamatis, D., Bertsch, J., Ovchinnikova, G., Katta, H. Y., Mojica, A., . . . Reddy, T. (2019). Genomes OnLine database (GOLD) v.7: updates and new features. Nucleic Acids Res, 47(D1), D649-D659. doi:10.1093/nar/gky977

Niess, J. H., Brand, S., Gu, X., Landsman, L., Jung, S., McCormick, B. A., ... & Littman, D. R. (2005). CX3CR1-mediated dendritic cell access to the intestinal lumen and bacterial clearance. *Science*, *307*(5707), 254-258.

Okawada, M., Koga, H., Larsen, S. D., Showalter, H. D., Turbiak, A. J., Jin, X., ... Teitelbaum, D. H. (2011). Use of enterally delivered angiotensin II type Ia receptor antagonists to reduce the severity of colitis. *Dig Dis Sci*, 56(9), 2553-2565. doi: 10.1007/s10620-011-1651-9.

Pamer, E. G. (2007). Immune responses to commensal and environmental microbes. Nat Immunol, 8(11), 1173-1178. doi:10.1038/ni1526

Park, J., Kim, M., Kang, S. G., Jannasch, A. H., Cooper, B., Patterson, J., & Kim, C. H. (2015). Short-chain fatty acids induce both effector and regulatory T cells by suppression of histone deacetylases and regulation of the mTOR-S6K pathway. *Mucosal Immunol*, 8(1), 80-93. doi: 10.1038/mi.2014.44.

Pluznick, J. L., Protzko, R. J., Gevorgyan, H., Peterlin, Z., Sipos, A., Han, J., . . . Caplan, M. J. (2013). Olfactory receptor responding to gut microbiota-derived signals plays a role in renin secretion and blood pressure regulation. Proc Natl Acad Sci U S A, 110(11), 4410-4415. doi:10.1073/pnas.1215927110

Romero, M., Toral, M., Robles-Vera, I., Sanchez, M., Jimenez, R., O'Valle, F., . . . Duarte, J. (2017). Activation of Peroxisome Proliferator Activator Receptor beta/delta Improves Endothelial Dysfunction and Protects Kidney in Murine Lupus. Hypertension, 69(4), 641-650. doi:10.1161/HYPERTENSIONAHA.116.08655

Santisteban, M. M., Qi, Y., Zubcevic, J., Kim, S., Yang, T., Shenoy, V., . . . Raizada, M. K. (2017). Hypertension-Linked Pathophysiological Alterations in the Gut. Circ Res, 120(2), 312-323. doi:10.1161/CIRCRESAHA.116.309006

Segata, N., Izard, J., Waldron, L., Gevers, D., Miropolsky, L., Garrett, W. S., & Huttenhower, C. (2011). Metagenomic biomarker discovery and explanation. Genome Biol, 12(6), R60. doi:10.1186/gb-2011-12-6-r60

Sharma, R. K., Yang, T., Oliveira, A. C., Lobaton, G. O., Aquino, V., Kim, S., . . . Raizada, M. K. (2019). Microglial Cells Impact Gut Microbiota and Gut Pathology in Angiotensin II-Induced Hypertension. Circ Res, 124(5), 727-736. doi:10.1161/CIRCRESAHA.118.313882

Sun, S., Lulla, A., Sioda, M., Winglee, K., Wu, M.C., Jacobs, D.R. Jr., . . . Meyer, K.A. (2019). Gut Microbiota Composition and Blood Pressure. Hypertension, doi: doi: 10.1161/HYPERTENSIONAHA.118.12109.

Takeshita, K., & Murohara, T. (2014). Does angiotensin receptor blockade ameliorate the prothrombotic tendency in hypertensive patients with atrial fibrillation? Breaking the vicious cycle. Hypertens Res, 37(6), 490-491. doi:10.1038/hr.2014.48

Tang, W. H., Wang, Z., Levison, B. S., Koeth, R. A., Britt, E. B., Fu, X., . . . Hazen, S. L. (2013). Intestinal microbial metabolism of phosphatidylcholine and cardiovascular risk. N Engl J Med, 368(17), 1575-1584. doi:10.1056/NEJMoa1109400

Tilg, H., & Kaser, A. (2011). Gut microbiome, obesity, and metabolic dysfunction. J Clin Invest, 121(6), 2126-2132. doi:10.1172/JCI58109

Toral, M., Robles-Vera, I., de la Visitación, N., Romero, M., Sánchez, M., . . . Duarte, J. (2019b). Role of the immune system in vascular function and blood pressure control induced by faecal microbiota transplantation in rats. *Acta Physiol (Oxf),* 227(1), e13285. doi: 10.1111/apha.13285.

Toral, M., Robles-Vera, I., De la Visitación, N., Romero, M., Yang, T., Sánchez, M., ... Duarte, J. (2019a). Critical role of the interaction gut microbiota-sympathetic nervous system in the regulation of blood pressure. *Front Physiol*, *10*, 231. doi.org/10.3389/fphys.2019.00231

Toral, M., Romero, M., Rodriguez-Nogales, A., Jimenez, R., Robles-Vera, I., Algieri, F., ... Duarte, J. (2018). Lactobacillus fermentum Improves Tacrolimus-Induced Hypertension by Restoring Vascular Redox State and Improving eNOS Coupling. Mol Nutr Food Res, e1800033. doi:10.1002/mnfr.201800033

Tsoporis, J., & Leenen, F. H. (1988). Effects of arterial vasodilators on cardiac hypertrophy and sympathetic activity in rats. Hypertension, 11(4), 376-386.

Tsuda, K., Shima, H., Ura, M., Takeda, J., Kimura, K., Nishio, I., & Masuyama, Y. (1988). Protein kinase C-dependent and calmodulin-dependent regulation of neurotransmitter release and vascular responsiveness in spontaneously hypertensive rats. J Hypertens Suppl, 6(4), S565-567.

Vaishnava, S., Behrendt, C. L., Ismail, A. S., Eckmann, L., & Hooper, L. V. (2008). Paneth cells directly sense gut commensals and maintain homeostasis at the intestinal host-microbial interface. Proc Natl Acad Sci U S A, 105(52), 20858-20863.

Vera, R., Jimenez, R., Lodi, F., Sanchez, M., Galisteo, M., Zarzuelo, A., . . . Duarte, J. (2007). Genistein restores caveolin-1 and AT-1 receptor expression and vascular function in large vessels of ovariectomized hypertensive rats. Menopause, 14(5), 933-940. doi:10.1097/GME.0b013e31802d9785

Vora, P., Youdim, A., Thomas, L. S., Fukata, M., Tesfay, S. Y., Lukasek, K., . . . Abreu, M. T. (2004). Beta-defensin-2 expression is regulated by TLR signaling in intestinal epithelial cells. J Immunol, 173(9), 5398-5405.

Wang, Q., Garrity, G. M., Tiedje, J. M., & Cole, J. R. (2007). Naive Bayesian classifier for rapid assignment of rRNA sequences into the new bacterial taxonomy. Appl Environ Microbiol, 73(16), 5261-5267. doi:10.1128/AEM.00062-07

Wengrower, D., Zanninelli, G., Latella, G., Necozione, S., Metanes, I., Israeli, E., . . . Goldin, E. (2012). Losartan reduces trinitrobenzene sulphonic acid-induced colorectal fibrosis in rats. Can J Gastroenterol, 26(1), 33-39.

Wilck, N., Matus, M. G., Kearney, S. M., Olesen, S. W., Forslund, K., Bartolomaeus, H., . . . Muller, D. N. (2017). Salt-responsive gut commensal modulates TH17 axis and disease. Nature, 551(7682), 585-589. doi:10.1038/nature24628

Yang, J. Y., Lee, Y.S., Kim, Y., Lee, S.H., Ryu, S., Fukuda, S., … Kweon, M. N. (2017) Gut commensal Bacteroides acidifaciens prevents obesity and improves insulin sensitivity in mice. *Mucosal Immunol*, 10(1), 104-116. doi: 10.1038/mi.2016.42.

Yang, T., Aquino, V., Lobaton, G. O., Li, H., Colon-Perez, L., Goel, R., ... & Pepine, C. J. (2019). Sustained Captopril-Induced Reduction in Blood Pressure Is Associated With Alterations in Gut-Brain Axis in the Spontaneously Hypertensive Rat*Journal of the American Heart Association*, *8*(4), e010721. doi:10.1161/JAHA.118.010721 Símb

Yang, T., Santisteban, M. M., Rodriguez, V., Li, E., Ahmari, N., Carvajal, J. M., . . . Mohamadzadeh, M. (2015). Gut dysbiosis is linked to hypertension. Hypertension, 65(6), 1331-1340. doi:10.1161/HYPERTENSIONAHA.115.0531

Zarzuelo, M. J., Jimenez, R., Galindo, P., Sanchez, M., Nieto, A., Romero, M., . . . Duarte, J. (2011). Antihypertensive effects of peroxisome proliferator-activated receptor-beta activation in spontaneously hypertensive rats. Hypertension, 58(4), 733-743. doi:10.1161/HYPERTENSIONAHA.111.174490

Zhou, H. W., Li, D. F., Tam, N. F., Jiang, X. T., Zhang, H., Sheng, H. F., . . . Zou, F. (2011). BIPES, a cost-effective high-throughput method for assessing microbial diversity. ISME J, 5(4), 741-749.

A

Phylum	WKY (n=6)	SHR (n=6)	SHR+Los (n=6)
Firmicutes	72.6 ± 5.0	86.4 ± 1.4*	74.8 ± 4.3#
Proteobacteria	11.0 ± 4.8	5.8 ± 1.4	7.5 ± 2.3
Actinobacteria	6.1 ± 1.0	3.5 ± 0.6*	4.4 ± 1.2
Bacteroidetes	5.1 ± 1.4	1.7 ± 0.3*	7.7 ± 1.5#
Verrucomicrobia	1.9 ± 0.6	0.8 ± 0.3	2.5 ± 1.2

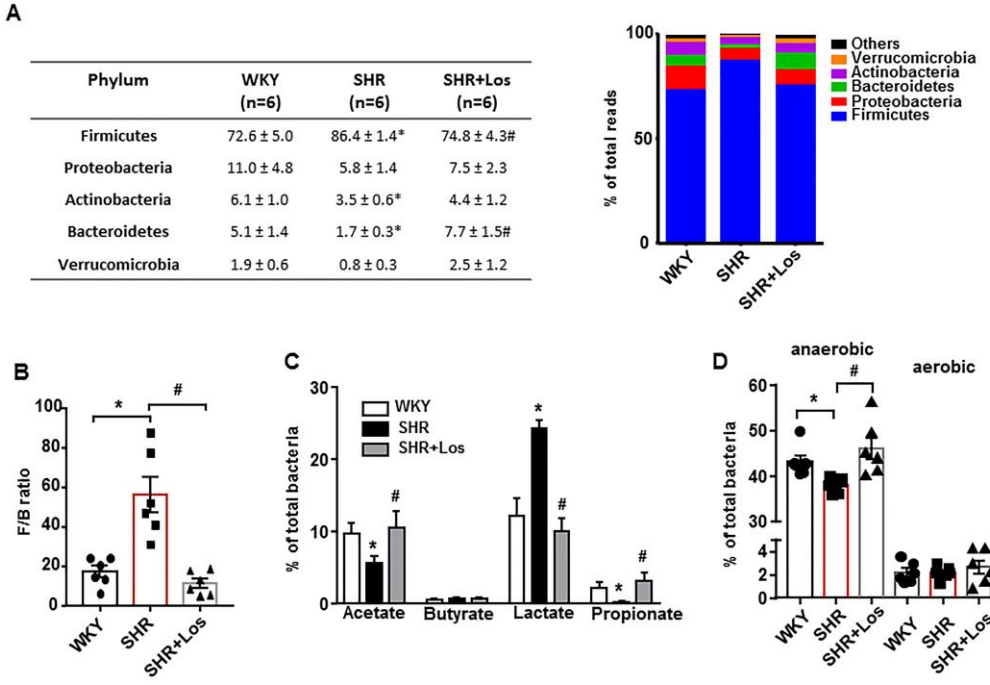

Figure 1

Figure 1. Losartan (Los) induces different behaviours of the gut microbiota of spontaneously hypertensive rats (SHR). Faecal samples were collected and bacterial 16S ribosomal DNA was amplified and sequenced to analyse the composition of microbial communities. Phylum breakdown of the 5 most abundant bacterial communities in the faecal samples obtained from all experimental groups (**A**). The *Firmicutes/Bacteroidetes* ratio (F/B ratio) was calculated as a biomarker of gut dysbiosis (**B**). Relative proportions of acetate-, butyrate-, lactate-, and propionate-producing bacteria (**C**). Anaerobic and aerobic bacteria expressed as relative proportions (**D**) in the gut microbiota in Wistar Kyoto rats (WKY), untreated SHR (SHR) and SHR treated with losartan (SHR-Los). Values are expressed as mean ± SEM (n = 6). *P< 0.05 significant differences compared with WKY rats. #P< 0.05 significant differences compared with the untreated SHR.

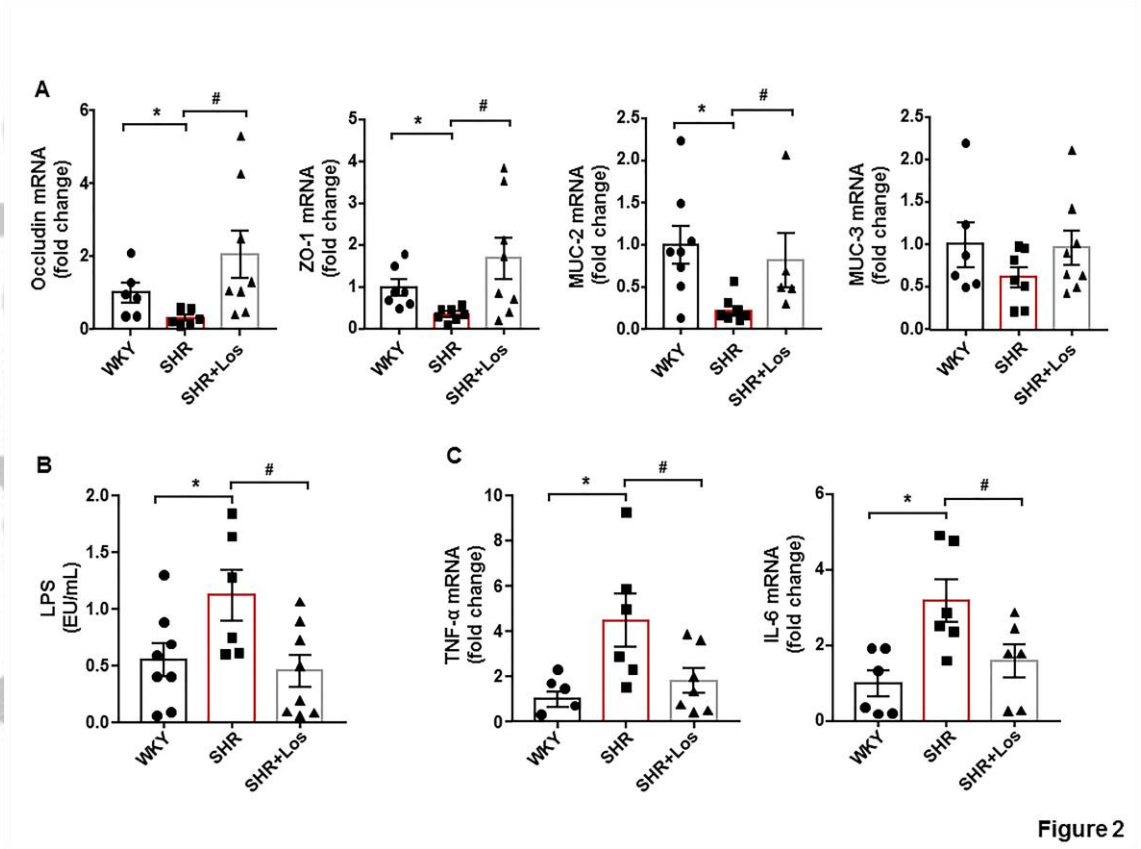

Figure 2. Losartan (Los) induces improvement of gut inflammation and permeability in spontaneously hypertensive rats (SHR). Colonic mRNA levels of occludin, zonula occludens-1 (ZO-1), mucin (MUC)-2, and MUC-3 (**A**). Plasma endotoxin concentrations (endotoxin units/mL (EU/mL)) (**B**). Pro-inflammatory cytokines, tumor necrosis factor-α (TNF-α) and interleukin (IL)-6 (**C**) in Wistar Kyoto rats (WKY), untreated SHR (SHR) and SHR treated with losartan (SHR-Los). Values are expressed as mean ± SEM (n = 8). *P< 0.05 significant differences compared with WKY rats. #P< 0.05 significant differences compared with the untreated SHR rats.

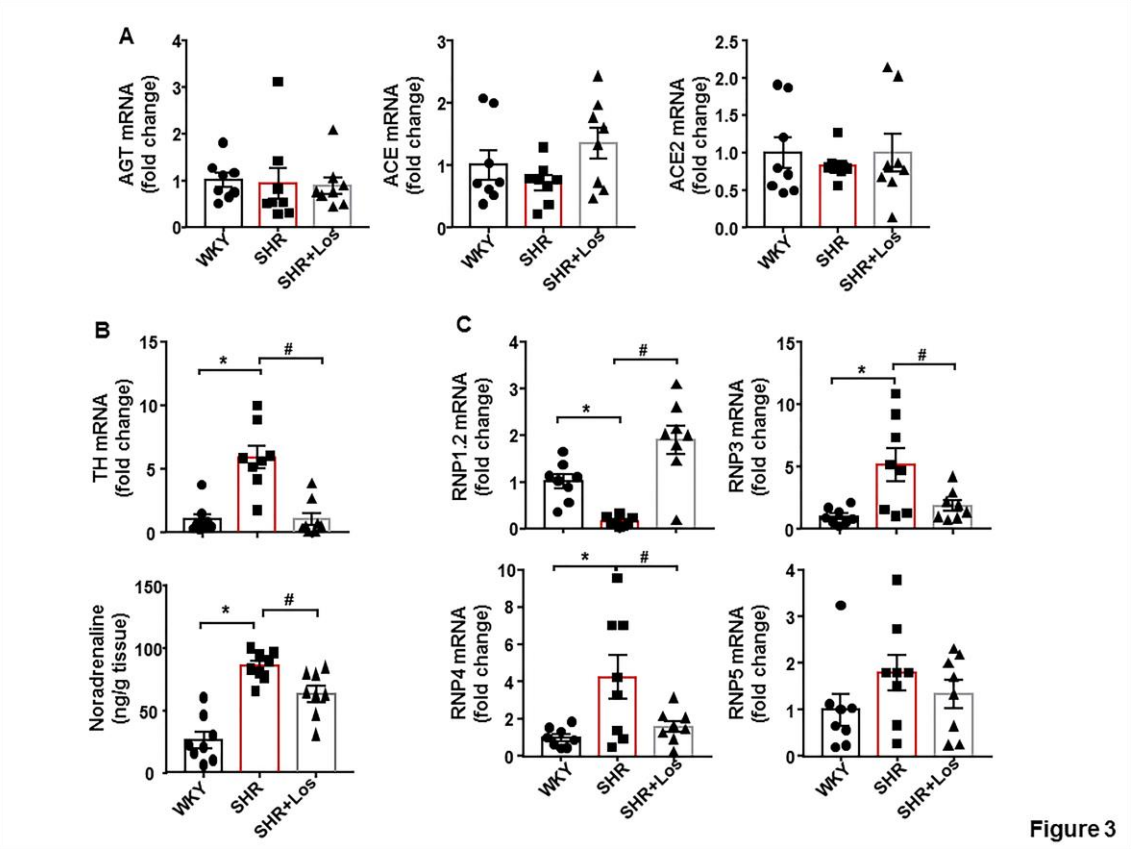

Figure 3. Losartan (Los) induces improvement of α-defensins production and gut sympathetic tone in spontaneously hypertensive rat (SHR). mRNA levels of several renin angiotensin system such as angiotensinogen (AGT), angiotensin-converting enzyme (ACE) and ACE2 (**A**). mRNA levels of tyrosine hydroxylase (TH) expression and noradrenaline content (**B**). mRNA levels of α-defensins (RNP1.2, RNP3, RNP4, and RNP5) in colon from Wistar Kyoto rats (WKY), untreated SHR (SHR) and SHR treated with losartan (SHR-Los). Values are expressed as mean ± SEM. *P< 0.05 significant differences compared with WKY. #P< 0.05 significant differences compared with the untreated SHR.

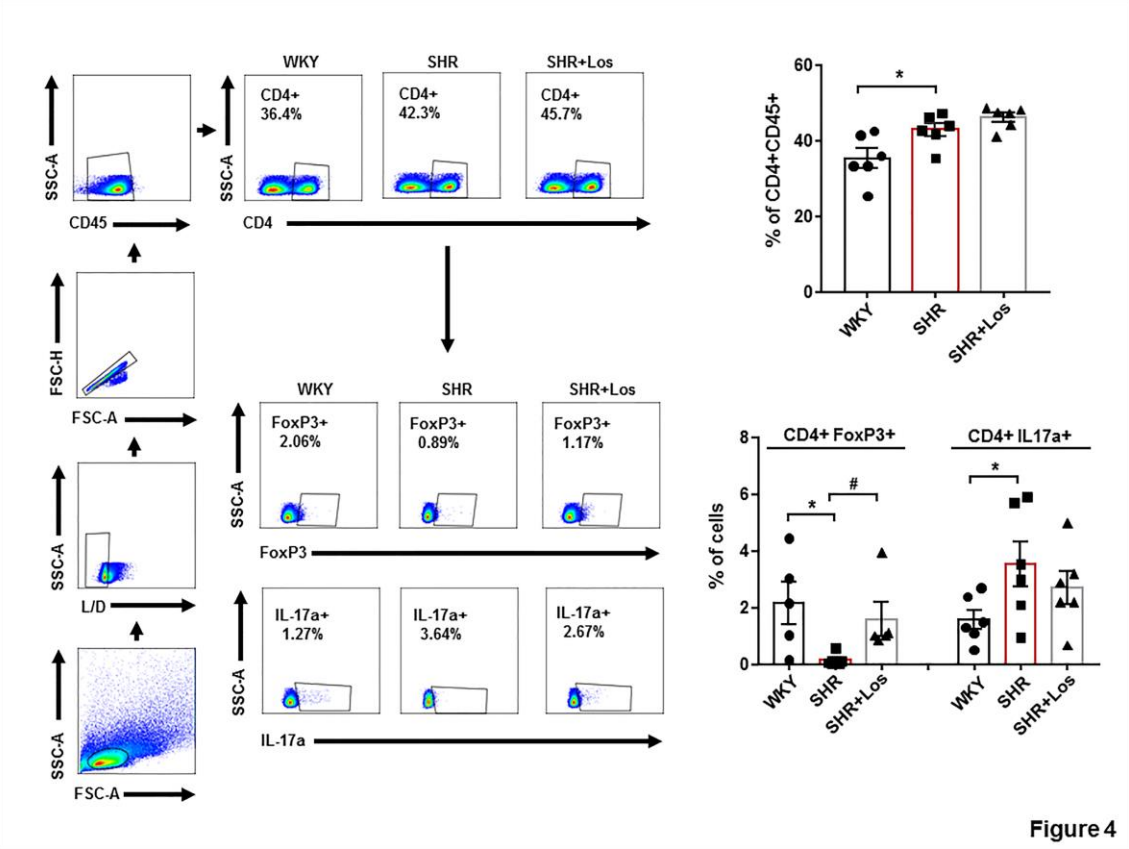

Figure 4. Losartan (Los) induces changes in T-cell polarization in mesenteric lymph nodes in spontaneously hypertensive rats (SHR). Total T cells (CD4+CD45+), regulatory T cells (Treg; CD4+ FoxP3+), and T helper (Th)-17 (CD4+ IL17a+) cells measured in mesenteric lymph nodes in Wistar Kyoto rats (WKY), SHR and SHR treated with losartan (SHR-Los). Values are expressed as mean ± SEM. *P< 0.05 significant differences compared with WKY. #P< 0.05 significant differences compared with untreated SHR.

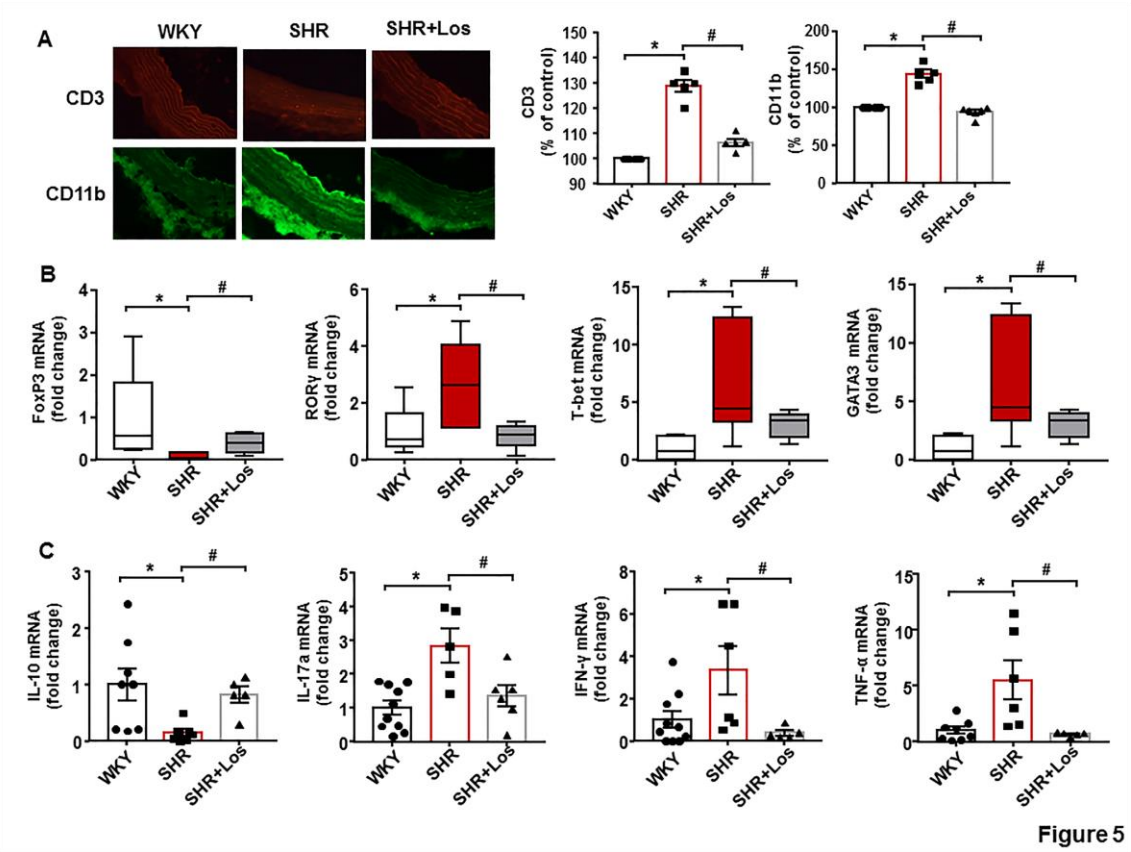

Figure 5. Losartan (Los) induces improvement of macrophage and T cell infiltration in vascular wall from spontaneously hypertensive rats (SHR). Pictures on the top show aortic T cell infiltration measured by immunostaining of CD3 (red fluorescence). Pictures on the bottom show aortic macrophage infiltration measured by immunostaining of CD11b (green fluorescence) (x 400 magnification). Data are represented as mean ± SEM of the red or green fluorescence (**A**). T-cells infiltration in aortas from all experimental groups measured by mRNA levels of regulatory T cells (Treg; FoxP3), T helper (Th)17; RORγ), Th1 (T-bet), and Th2 (GATA-3) cells (**B**). mRNA levels of interleukin (IL)-10, IL-17a, interferon-γ (IFN-γ), and tumor necrosis factor-α (TNF-α) (**C**) in aortas from Wistar Kyoto rats (WKY), SHR and SHR treated with losartan (SHR-Los). Values are expressed as mean ± SEM. *P< 0.05 significant differences compared with WKY. #P< 0.05 significant differences compared with untreated SHR.

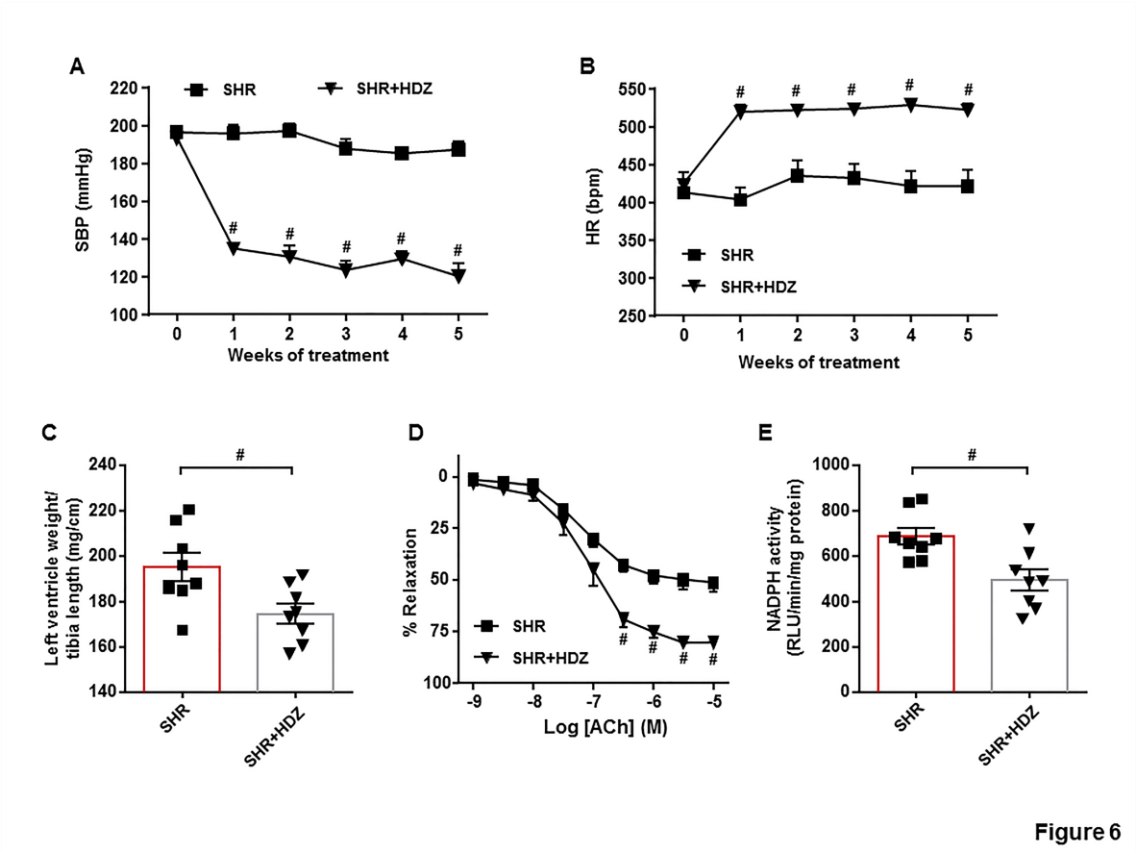

Figure 6. Protective effects of hydralazine (HDZ) in endothelial dysfunction and hypertension in spontaneously hypertensive rats (SHR). Time course of systolic blood pressure (SBP, **A**) and heart rate (HR, **B**) measured by tail-cuff plethysmography in SHR treated with the hydralazine or saline. Morphological data from the left ventricle (**C**). Endothelium dependent relaxation induced by acetylcholine (ACh) in aortas precontracted by phenylephrine (**D**) and NADPH oxidase activity measured by lucigenin enhanced chemiluminescence (**E**) in aorta from SHR and SHR+HDZ groups. Values are represented as means ± SEM (n = 8). #P< 0.05 significant differences compared with untreated SHR.

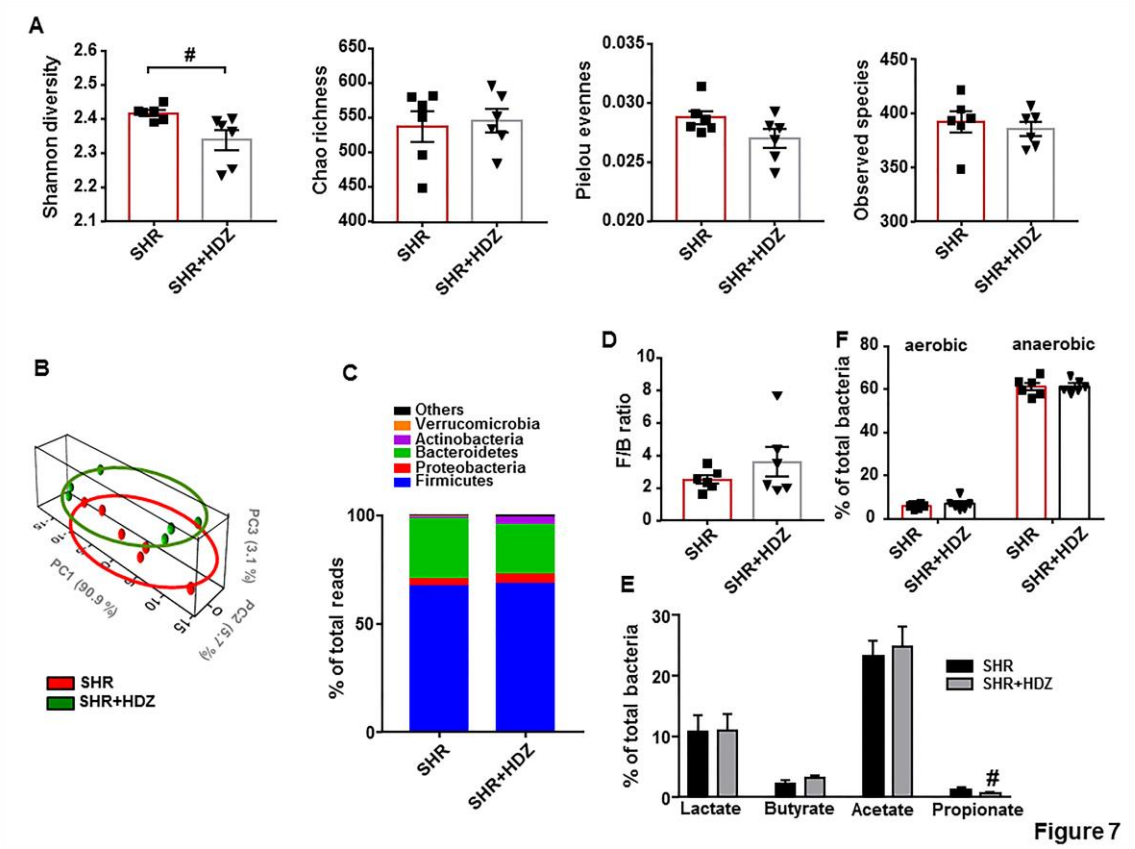

Figure 7

Figure 7. Hydralazine (HDZ) does not induce changes in the gut microbiota composition in spontaneously hypertensive rat (SHR). The microbial DNA from faecal samples was analysed by 16S rRNA gene sequencing. To evaluate general differences of microbial composition amongst all experimental groups, diversity, richness, evenness, and observed species (**A**) were examined. Principal coordinate analysis in the gut microbiota from all experimental groups (**B**). Phylum breakdown of the 5 most abundant bacterial communities in samples from all groups (**C**). The *Firmicutes/Bacteroidetes* ratio (F/B ratio) was calculated as a biomarker of gut dysbiosis (**D**). Relative proportions of anaerobic and aerobic bacteria (**F**), and lactate-, butyrate-, acetate- and propionate-producing bacteria expressed as relative proportions (**E**) in the gut microbiota in all experimental groups are shown. Values are represented as mean ± SEM. #P< 0.05 significant differences compared with untreated SHR.

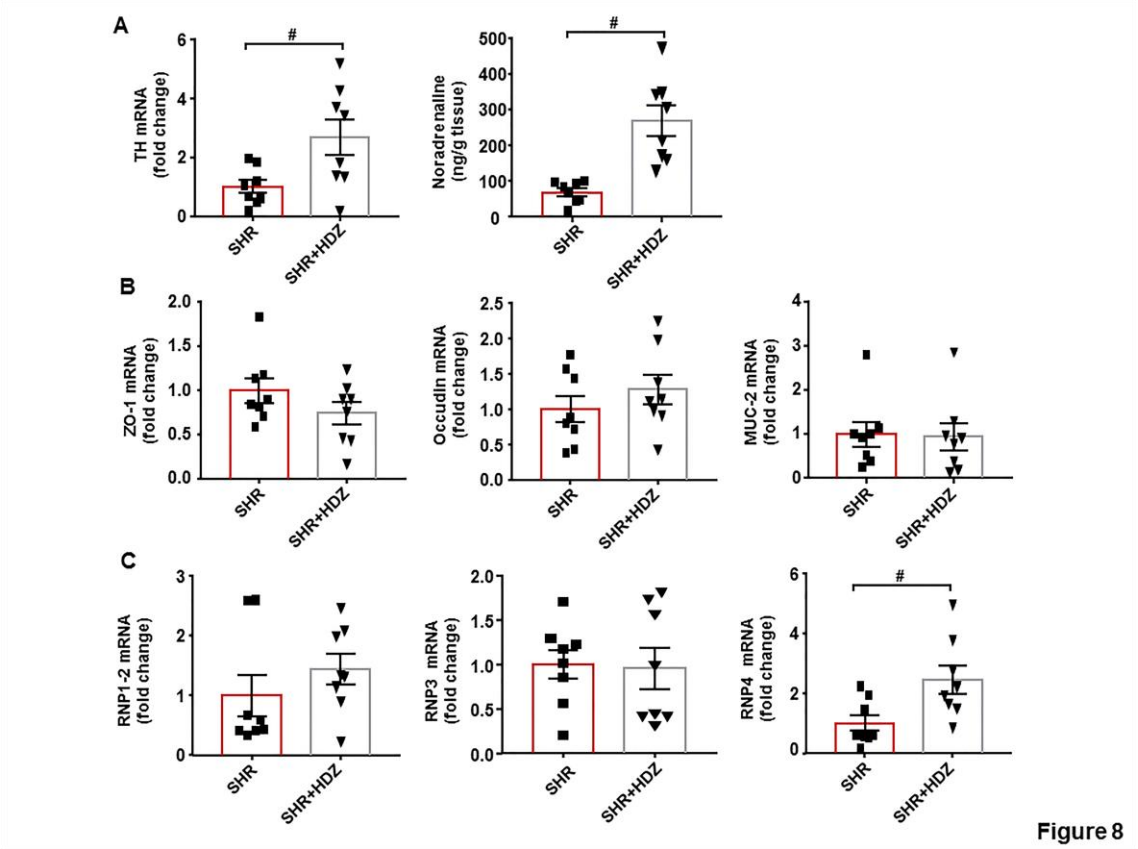

Figure 8. Effects of hydralazine (HDZ) on the sympathetic tone and gut integrity in spontaneously hypertensive rats (SHR). Colonic mRNA levels of tyrosine hydroxylase (TH) and noradrenaline levels (**A**). Zonula occludens-1 (ZO-1), occluding, mucin (MUC)-2 (**B**), and α-defensins, RNP1.2, RNP3, and RNP4 (**C**) measured by RT-PCR in the colon from all experimental groups. Values are represented as mean ± SEM. #P< 0.05 significant differences compared with untreated SHR.

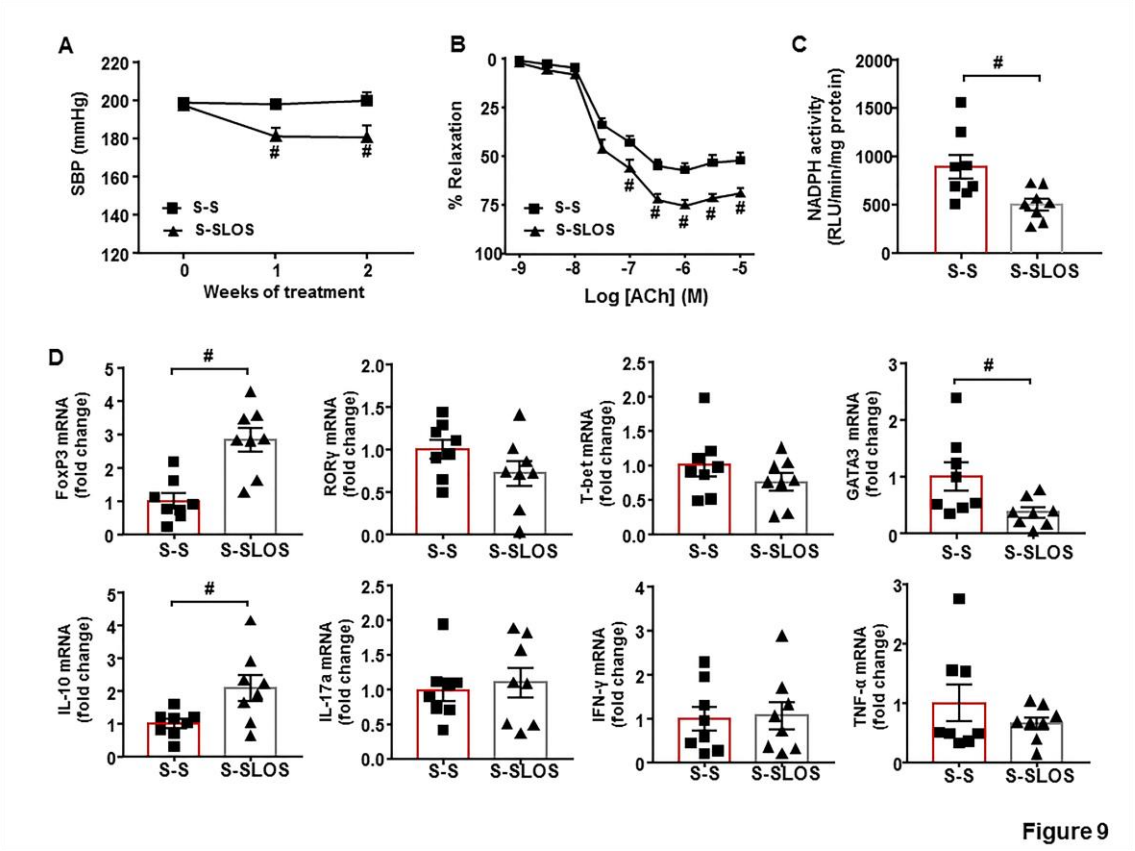

Figure 9. Effects of faecal microbiota transplantation from spontaneously hypertensive rat (SHR)-losartan to SHR on vascular function in SHR. Time course of systolic blood pressure (SBP), measured by tail-cuff plethysmography, in SHR with stool transplant from SHR (S-S) or from SHR treated with losartan (S-SLOS, **A**). Endothelium-dependent relaxation induced by acetylcholine (ACh) in aortas pre-contracted by phenylephrine (**B**) and NADPH oxidase activity measured by lucigenin-enhanced chemiluminescence in aorta from S-S, S-SLOS (**C**). mRNA levels of regulatory T cells (Treg; FoxP3), T helper (Th)-17; RORγ), Th1 (T-bet), and Th2 (GATA-3) cells and mRNA levels of interleukin (IL)-10, IL-17a, interferon-γ (IFN-γ), and tumor necrosis factor-α (TNF-α) (**D**) in aortas from S-S and S-SLOS groups. Values are represented as mean ± SEM. #P< 0.05 significant differences compared with S-S group.

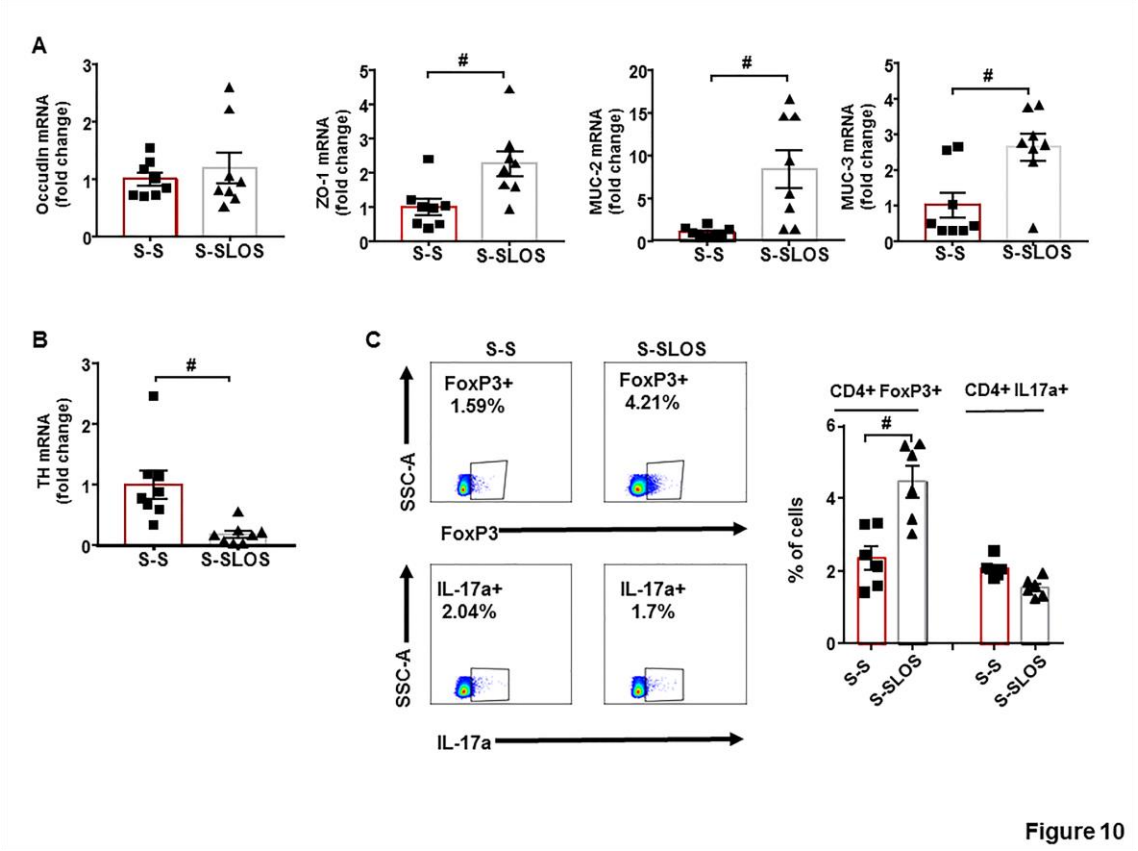

Figure 10. Effects induced by faecal microbiota transplantation from spontaneously hypertensive rats (SHR)-losartan on gut integrity and gut sympathetic activity. mRNA levels of occludin, zonula occludens-1 (ZO-1), mucin (MUC)-2, MUC-3 (**A**), and tyrosine hydroxylase (TH, **B**) measured by RT-PCR in colon from all experimental groups. Regulatory T cells (Treg) and T helper (Th)-17 measured in mesenteric lymph nodes from all S-S and S-SLOS groups by flow cytometry. Values are represented as mean ± SEM. #P< 0.05 significant differences compared with S-S group.